

Open-Vocabulary Temporal Action Detection with Off-the-Shelf Image-Text Features

Vivek Rathod
rathodv@google.com

Bryan Seybold
seybold@google.com

Sudheendra Vijayanarasimhan
svnaras@google.com

Austin Myers
aom@google.com

Xiuye Gu
xiuyegu@google.com

Vighnesh Birodkar
vighneshb@google.com

David A. Ross
dross@google.com

Google Research
Mountain View, CA
USA

Abstract

Detecting actions in untrimmed videos should not be limited to a small, closed set of classes. We present a simple, yet effective strategy for open-vocabulary temporal action detection utilizing pretrained image-text co-embeddings. Despite being trained on static images rather than videos, we show that image-text co-embeddings enable open-vocabulary performance competitive with fully-supervised models. We show that the performance can be further improved by ensembling the image-text features with features encoding local motion, like optical flow based features, or other modalities, like audio. In addition, we propose a more reasonable open-vocabulary evaluation setting for the ActivityNet data set, where the category splits are based on similarity rather than random assignment.

1 Introduction

Humans can learn to recognize new objects from only a few examples and/or simple descriptions because they can apply prior experience to do so. Recent Image-Text Co-Embedding (ITCE) models, such as CLIP [32], Align [18], and Basic [31], demonstrate one path to achieve this goal in computer vision. These models learn a joint representation for images

and texts using contrastive learning on Internet-scale image-text pairs and are able to capture the rich information present in text descriptions such as objects, actions, human-object interactions, and object-object relationships. ITCE features have demonstrated excellent open-vocabulary and zero-shot transfer performance on various image classification tasks without the need for additional fine-tuning or manually-annotated datasets. Recent works apply ITCE features to downstream open-vocabulary tasks such as object detection [13, 48], action recognition [19, 25, 41] and—relatively underexplored—temporal action detection [19].

In this paper, we consider open-vocabulary Temporal Action Detection (**TAD**). We show that open-vocabulary TAD models using ITCE features outperform fully-supervised models from a year ago and approach the performance of concurrent work. TAD requires detecting and classifying actions in untrimmed videos. TAD is usually done in a fully-supervised setting: the training set contains videos annotated with the 3-tuples of segment start, end, and action labels. In the open-vocabulary setting, segments with a subset of action labels for evaluation are held out and unseen during the training phase then predicted during evaluation. We decouple the problem into learning to detect class-agnostic temporal segments and classifying the detected segments. Classification of video segments can be remarkably effective and straightforward using ITCE by simply averaging image features within each detected segment and comparing to the text embedding of each class label. We demonstrate open-vocabulary performance that is comparable to fully-supervised TAD and outperforms open-vocabulary models from the literature when utilizing strong image-text co-embedding features, such as from CLIP [32], Align [18] and BASIC [31].

To summarize, our main contributions are:

- A method on open-vocabulary temporal action detection that outperforms a large number of fully-supervised models.
- Detailed evaluation of different image-text co-embedding features for both class agnostic action detection and open-vocabulary action classification.
- A survey of features to complement image-text co-embedding features for class-agnostic detection to identify synergistic features that improve open-vocabulary performance.
- A rationally designed “Smart split” for open-vocabulary temporal action detection on ActivityNet that leverages the class hierarchy for more meaningful evaluation.

2 Related Work

Open-vocabulary image-text co-embedding models and object detection. Pre-training on large manually-annotated classification datasets such as Imagenet [9] or JFT [38] is effective for learning image features that generalize to downstream tasks with limited training data, but manual annotation limits the size of datasets for training. Recent work on ITCEs such as CLIP [32], Align [18] and BASIC [31] instead use contrastive training. The joint embedding spaces these models learn from weakly-labeled, Internet-scale datasets enabled downstream open-vocabulary classification tasks at high accuracy without requiring fine-tuning or manual annotation.

Open-vocabulary object detection aims to detect objects of unseen classes by learning to generalize from annotated objects [5, 33, 53], textual descriptions [21] or captions [48]. Recent work, such as [13, 48], decoupled the problem into learning class-agnostic proposal generators followed by open-vocabulary image classification using ITCE features and brought performance closer to fully-supervised detection than previous methods.

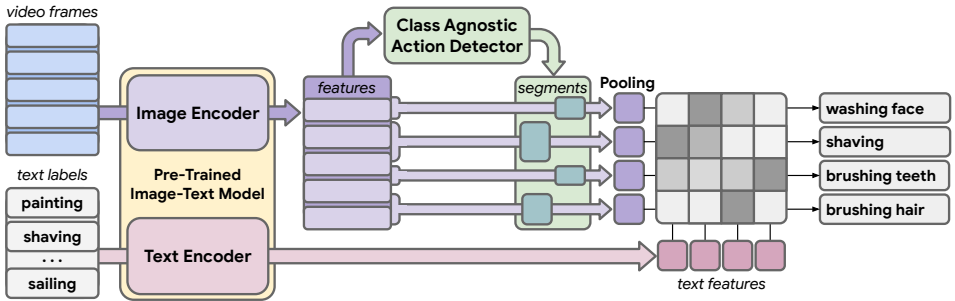


Figure 1: Overview of Open-Vocabulary Temporal Action Detection. Video frames are processed by a pre-trained image encoder. These features or others are passed to a class-agnostic detector to detect temporal segments. Within each segment, the image features are pooled to form a segment feature. Finally, the segment feature is compared to the text feature of each class label of interest passed through a text encoder. The class labels during inference may be entirely novel.

Image-text co-embedding models for video and temporal action detection. Several recent arXiv papers [19, 25, 41] leverage pre-trained CLIP [32] features for video retrieval, action recognition and action localization. While [25, 41] fine-tune the CLIP [32] model end-to-end for video tasks, [19] focuses on efficiently adapting image features to videos tasks through temporal aggregation and gradient-based prompt-engineering.

TAD consists of detecting and classifying actions from untrimmed videos. TAD approaches can be roughly categorized as weakly-supervised methods that only train on video class labels [17, 29, 40], self-contained methods [8, 24, 35, 49, 52] that are trained end-to-end to predict and classify segments and two-stage methods [23, 42, 46, 50] that use various approaches to predict candidate segments and use state-of-the-art action classifiers [44] to classify them. However, all these approaches use the same fixed vocabulary of actions for both training and testing and are fully supervised.

A few recent work attempt open-set TAD [43] and open-vocabulary TAD [19]. In [43], the authors introduce the open-set TAL problem where a single 'unknown' label is introduced to model missing classes. Both our model and [19] consider the more general open-vocabulary TAD problem and use two-stage models that replace the supervised classifier with a ITCE feature comparison. Our work differs from [19] along several axes: we compare ITCE features, we test features that can complement ITCE features, we explore more dataset splits, and we do not do prompt engineering. Through extensive experiments, we outperform other open-vocabulary TAD models [19] by a large margin and approach the performance of fully supervised models from recent literature by using strong ITCE features.

3 Method

3.1 Class-Agnostic Detection and Open-Vocabulary Classification

To detect temporal actions, we first produce class-agnostic segment detections in each video and follow-up with open-vocabulary classification as shown in Figure 1. We begin by extracting detection features, $f_t^d = F^d(X_t)$, and open-vocabulary features, $f_t^{ov} = F^{ov}(X_t)$,

from video frames, $X_{1..T}$, where F^d and F^{ov} are pre-trained models. Both may be the same model; F^{ov} is always an ITCE model; and both are applied with temporal windowing to produce one output feature per second of video. Following common TAD practices [8, 23, 24, 35, 46, 49, 52], we detect segments from the pre-extracted features using an architecture similar to object detection, $S = D(f_{1..T}^d)$. To classify each segment, we pool the ITCE features within each segment along each dimension, $f_S^{ov} = \mathbb{E}_{t \in S}[f_t^{ov}]$, compute the ICTE features for the text labels, $f_Y^{ov} = F^{ov}(Y)$ where Y is the text of a class label, and then assign a class label that maximizes the softmax of the dot-product between the segment feature and text feature: $\text{argmax}(\text{softmax}(f_S^{ov} \cdot f_Y^{ov}))$.

As open-vocabulary TAD is a new area, we focus on a solid foundation evaluating off-the-shelf models and features. The novelty of our work is that ITCE features enable straightforward methods to outperform other open-vocabulary work and nearly match state-of-the-art, fully-supervised results without needing complicated tricks. We focus on using out-of-the-box detection models that achieve good performance on temporal action detection rather than relying on models that may be over-tuned to use specific input features and datasets common in the literature. More complicated models for open-vocabulary action detection should improve our results, but we leave that for future research because including more complicated models would make it difficult to communicate how effective simple models are with ITCE features.

3.2 Smart Split

Smart Split			
Shot put	Hammer throw	Long jump	Smoking a cigarette
Spinning	High jump	Vacuuming floor	Using the pommel horse
Camel ride	Playing racquetball	Hurling	Playing ice hockey
Kayaking	Wakeboarding	Rafting	Longboarding
Assembling bicycle	Zumba	Belly dance	Painting furniture
Playing accordion	Playing flauta	Playing violin	Tennis serve with ball bouncing
Skiing	Playing congas	Drum corps	Futsal
Playing beach volleyball	Doing karate	Playing badminton	Getting a haircut
Playing kickball	Doing motocross	Cutting the grass	Making an omelette
Preparing salad	Grooming horse	Washing face	Blowing leaves
Shaving legs	Plataform diving	Polishing shoes	Mixing drinks
Painting fence	Roof shingle removal	Clipping cat claws	Windsurfing
River tubing	Waterskiing		

Table 1: ActivityNet Smart 75/25 Split. The strings listed are the ActivityNet labels held out for evaluation. This split is designed so that the classes in evaluation are similar to classes in the training set.

Open-vocabulary detection is commonly evaluated in the literature by separating different classes of a well-known data set into new training and evaluation splits [13, 19, 48]. One simple way to split the data is to randomly select a subset of all classes to hold out. Random splits artificially limit open-vocabulary performance compared to fully-supervised methods because it breaks the distribution match training and evaluation sets. In contrast, fully-supervised methods are generally evaluated with matching distributions.

Even defining action boundaries in time is notoriously difficult, so care is always needed to ensure TAD evaluations are meaningful. The two most common temporal action detection data sets, ActivityNet [11] and Thumos [16] disagree on the length of actions with even the same label by an order of magnitude, and data set creators need to defend whether the label

annotators are able to be consistent [1]. With a random split, many errors will simply occur because the evaluation set is out of domain for the model, which are uninteresting errors.

To address the mismatch, we propose a new split of the ActivityNet dataset that is designed so that classes in evaluation are similar to classes in the training set. Table 1 shows the 25% of the classes selected to be in the evaluation split with the remaining 75% of the classes used for training. We do this to ensure that for each class in the evaluation set, some class in the training set has similar boundaries by taking neighbors from the ActivityNet class ontology. We hope that this split is useful to the TAD community for evaluating open-vocabulary TAD going forward..

3.3 Complementary Features

ITCE features based on images will not perfectly encode video because they operate on each frame individually. One possible improvement is to adapt ITCEs to take multiple frames into account [19, 25, 41], but these methods risk overfitting and have not yet been proven to reliably encode temporal information. In contrast, we include time-tested features such as I3D_RGB and I3D_FLOW [7] that have been shown to encode temporal information, or explicit audio features [14, 39]. These features can establish a meaningful baseline for evaluating future work to produce new video features.

4 Experiments

4.1 Data sets and splits

Data sets: We focus on the two most common temporal action detection data sets in the literature: ActivityNet 1.3 [11] and Thumos14 [16]. We use the entire Thumos data set and the 90% of ActivityNet that is still accessible. We verify that our comparable models using CLIP B/16 embeddings achieve comparable performance to a recent paper using the same features [19] (see results) despite any change in the data.

Random splits: For each data set, we create two sets of random splits: 12 random splits with 75% of the data in the training set and 25% held out for evaluation; as well as another 4 random splits with 50% in the training set and 50% held out for evaluation. The exact labels used for the evaluation set of each split are provided in the supplemental. (We compared class-agnostic detection performance on our splits versus the 10 random splits from [19] and found them virtually identical. See supplemental.) Unless otherwise noted, we present numbers as mean \pm standard error of the mean when presenting results on random splits. If one video has labels from both the training and evaluation splits, the same video appears in both splits, but with only the labels in that split. This configuration is challenging because true-positives for the training set hurt performance during evaluation, but accurately maps onto real uses of open-vocabulary detection.

Smart split: As described in 3.2, intelligently selecting an open-vocabulary split with related concepts in the training and evaluation sets is a more meaningful evaluation than mismatched concepts. We propose the **Smart split** for ActivityNet based on the provided class hierarchy with 25% of the labels in the evaluation set. We created the Smart split by taking pairs of neighboring leaf nodes from the hierarchy and ensuring that one was held out for evaluation and the other was used for training. Based on a subjective assessment, we only chose pairs that were perceptually similar. (E.g. “Playing rubik cube” is visually distinct from all other

classes, and would not be used in a pair.) We provide the exact labels used for the evaluation set of the Smart split in the supplemental and hope future work will report on this split to give a meaningful comparison without needing to test as many split combinations.

We do not make a Smart split for Thumos as there is no class hierarchy and the data set contains only 20 classes.

4.2 Models

We use two different models on the two different data sets because we find that different out-of-the-box detection models perform much better on the fully supervised temporal action detection task (see supplemental for model details).

For ActivityNet, we use a DeTr [6] detection head on top of a stacked-hourglass [30]-style feature extractor. The feature extractor stacks 1D convolution residual blocks with LayerNorm [4] and ReLU activations in a U-Net pattern of downsampling and upsampling. Additional residual connections are passed between blocks at the same resolution to avoid loss of temporal information. Four residual U-Net stacks are applied in turn before the detection head. For Thumos, we use a CenterNet [10] detection head on top of the same style of feature extractor. Both detection heads are adapted for 1D detection by treating all proposals and ground truth segments as boxes with a fixed height of one. The CenterNet code is adapted from [15]. On the fully-supervised TAL task, these models achieve competitive performance each data set using TSP [2] features: ActivityNet, 28% mAP Avg @ IoU 0.5:0.95:0.05 (without using external, whole-video classification); Thumos, 52% mAP @ IoU 0.5. The TSP features are trained on all 200 classes of ActivityNet and all 20 of Thumos, so we cannot evaluate TSP features for open-vocabulary performance.

Key hyperparameters for the models and optimization: DeTr: transformer heads is set to 16, transformer dimensions are 1024, segment classifier’s hidden layer size is 1024, maximum number of proposals is set to 64, background class weight is set to 3.0, weight decay is set to 0.0005 and the positional encoding is learned. CenterNet: maximum number of segments is set to 512, scale loss weight is 0.1, heatmap head dimensions is set to 256. Residual Feature Extractor: base hidden dimensions is set to 512, resolutions is set to 5, number of stacked U-Nets is set to 4, kernel size is set to 5. We use the Adam optimizer with a learning rate of 0.0001 and train for 20,000 steps. See supplemental for additional details.

4.3 Features

We use the following features: I3D_RGB and I3D_FLOW [7] features trained on Kinetics [20]; VIVIT [3] features trained on Kinetics; VGGISH [14] features trained on AudioSet [12]; YAMNET [39] features pre-trained on AudioSet; ALIGN [18] features trained on the Align data set; BASIC [31] features trained on Align+JFT [38] data sets; MBT-a [27] trained on AudioSet [12]; MBT-v [27] trained on Kinetics [20]; and CLIP [32] B/16, B/32, and L/14 features trained on WebImageText. We extract each feature at 1 FPS on both data sets using a sliding window for features that take more than 1 second of input.

We do not use video-text co-embeddings because the performance of related models was worse than image-text models without finetuning (see supplemental and literature [28]). Most video-text models are still fine-tuned for specific tasks due a lack of large scale video-text datasets [25, 41], and we evaluate other fine-tuned video transformer features [3, 26].

Features	Setup	ActivityNet			Thumos		#params	
		Top-1	Top-5	Smart split Top-1	Top-1	Top-5	Image tower	Text tower
2016 ANet winner [44]	Supervised	88.1	-	-	-	-	-	-
CLIP ViT-B/32 [32]	Open-Vocab	65.38	89.26	65.95	61.61	90.11	87 M	63 M
CLIP ViT-B/16 [32]	Open-Vocab	71.29	92.41	66.32	64.26	93.58	87 M	63 M
CLIP ViT-L/14 [32]	Open-Vocab	78.2	95.74	75.38	70.59	97.05	303 M	123 M
ALIGN [18]	Open-Vocab	77.92	94.53	76.06	42.83	70.35	632 M	632 M
BASIC [31]	Open-Vocab	88.73	97.52	88.29	81.86	98.2	2.4 B	670 M

Table 2: Open-Vocabulary Classification of Ground Truth Segments. We present Top-1 and Top-5 classification accuracies on ground truth segments by comparing pooled features to text label embeddings for ActivityNet (original 200-class split and 50-class Smart split) and Thumos (the original 20-class split). We also list the number of parameters in the image and text towers of each image-text model.

4.4 ITCE Features Empower Open-Vocabulary Action Classifiers

To motivate this work, we first test how powerful ITCE features are for ground truth segment classification. For each ground truth segment, we pool the 1 FPS features from different models then assign the label from the closest text embedding. In general, the performance on ground truth segments in Table 2 scales with model size for the original splits and the Smart split. The Smart split is as difficult to classify as the original data. The performance of the BASIC image-text co-embeddings exceeds the Top-1 accuracy of fully-supervised ActivityNet video classification models like [44] commonly used to do classification on top of temporal action proposal networks in recent literature. Using off-the-shelf ITCE features enable better classification than using the ActivityNet training data!

4.5 Class-Agnostic Detection

We evaluate our models for class-agnostic detection on random open-vocabulary splits of each data set to match the common open-vocabulary paradigm and the Smart split of ActivityNet. We present both an average of mean Average Precision (mAP) at different Intersection over Unions (IoUs) and average recall at N metrics for comparison to the literature, but emphasize that AP metrics are more appropriate: For open-vocabulary detection, the classifier cannot classify segments as background so these are detections, rather than merely proposals. Precision matters as much as recall for detections.

In Table 3, we find that ITCE features are effective for class-agnostic temporal detection. (These can be compared to fully-supervised temporal action detection in Table 4 and supplemental). As with ground truth classification performance, ITCE features from larger models perform better. The I3D_RGB + I3D_FLOW features commonly used in the TAD literature are also very good for class-agnostic detection. Audio features alone do surprisingly well, and recent video transformers trained for classification such as ViViT and MBT do surprisingly poorly. (In the supplemental, we show that doing fully supervised training with classification restores the expected order that modern ViViT and MBT do well while audio features alone are insufficient to classify visual actions.) The Smart split is typically 1-2% AP better than the average of random splits. This difference highlights that a major challenge for open-vocabulary temporal action detection is a difficulty recognizing segments of novel classes.

Because Thumos contains so few classes, evaluation on the held-out evaluation classes

Features	ActivityNet						Thumos			
	75/25 splits average (n=12)		Smart split		50/50 splits average (n=4)		75/25 splits average (n=12)		50/50 splits average (n=4)	
	AP@avg	AR@10	AP@avg	AR@10	AP@avg	AR@10	AP@avg	AR@10	AP@avg	AR@10
CLIP b/32 [32]	27.2 ± 1.0	41.3 ± 0.9	29.2	43.0	25.6 ± 0.4	38.6 ± 0.9	32.2 ± 7.7	14.3 ± 3.2	16.4 ± 4.5	8.1 ± 2.6
CLIP b/16 [32]	27.6 ± 1.0	42.4 ± 1.2	30.7	44.0	25.8 ± 0.7	40.0 ± 1.3	32.1 ± 8.0	14.1 ± 3.5	20.4 ± 4.0	9.8 ± 1.9
CLIP l/14 [32]	28.2 ± 0.8	42.5 ± 0.9	31.3	43.4	26.6 ± 0.6	40.1 ± 0.7	34.8 ± 7.9	15.6 ± 3.2	18.3 ± 5.7	8.7 ± 2.0
ALIGN [18]	27.8 ± 0.9	42.3 ± 0.8	30.3	43.0	26.1 ± 0.9	40.1 ± 1.0	31.7 ± 4.9	14.2 ± 3.3	20.9 ± 4.2	9.7 ± 2.3
BASIC [31]	28.8 ± 0.9	43.3 ± 0.8	32.0	44.9	27.0 ± 0.8	41.0 ± 1.1	33.7 ± 7.9	15.2 ± 3.5	20.2 ± 2.8	10.4 ± 2.2
I3D RGB+FLOW	28.4 ± 0.9	42.3 ± 0.8	30.4	43.1	26.5 ± 0.5	40.4 ± 0.7	38.6 ± 9.3	16.1 ± 3.9	26.9 ± 6.9	11.7 ± 3.0
I3D RGB [7]	27.2 ± 0.7	41.3 ± 0.7	30.7	43.8	25.1 ± 0.3	38.9 ± 0.3				
I3D FLOW [7]	28.3 ± 1.0	42.2 ± 1.0	29.6	42.5	25.6 ± 0.5	40.3 ± 0.1.3				
YAMNET [39]	22.7 ± 0.6	36.6 ± 0.6	25.5	40.1	20.9 ± 1.0	34.9 ± 0.1.7				
VGGISH [14]	23.0 ± 0.8	36.9 ± 0.9	25.0	38.8	21.3 ± 0.5	35.6 ± 1.1				
VIVIT [3]	22.4 ± 0.8	37.1 ± 1.1	24.8	40.0	20.0 ± 0.4	34.2 ± 1.1				
MBT-v [26]	23.5 ± 0.7	38.5 ± 0.8	25.6	40.8	21.8 ± 0.4	36.9 ± 0.9				
MBT-a [26]	18.1 ± 0.8	34.1 ± 1.0	20.0	35.1	17.9 ± 0.3	33.6 ± 0.5				

Table 3: Class-Agnostic Detection Results. Performance of the same class-agnostic detector architectures with different input features. On ActivityNet, mAP@Avg is mAP@0.5:0.05:0.95. On Thumos, mAP@avg is mAP@0.3:0.1:0.7. AR@10 is Average Recall at 10. Data is grouped as columns for 75/25 random splits (n=12) and Smart split, and 50/50 random splits (n=4). Aggregates are means ± standard error across splits. Some features were not tested on Thumos. See supplemental for additional metrics.

jumps by large amounts whenever a new class is learned (see figure in supplemental). Because some classes are harder to learn than others depending on the splits, the performance across splits has much larger variability for Thumos than for ActivityNet. The standard error is 10-times larger: 8% mAP for Thumos and 0.9% mAP for ActivityNet. The adoption of larger data sets in future work will hopefully decrease the variance in evaluations.

4.6 Open Vocabulary Temporal Action Detection

We evaluate the open-vocabulary temporal action detection performance of each ITCE feature in Table 4. We evaluate each feature two ways. We use the ITCE feature for both detections and classification, and we also use the ITCE feature for classification on top of I3D_RGB + I3D_FLOW detections. Using the same features and a similar architecture to BaselineIII from [19], our CLIP-b/16 results are slightly better (21.4 ± 0.7 vs 20.2). They fine-tune their CLIP-b/16 features on ActivityNet and perhaps that causes overfitting. Using BASIC features results in a substantial improvement in performance that substantially outperforms [19].

The Thumos data set is much more difficult. In our evaluation, which mimics expected use scenarios, true-positives for the training classes are false-positives during evaluation. This differs from the evaluation approach in [19] that splits each long video with multiple class labels, by an undescribed method, into short video clips with only one label and only evaluates on the subset of video clips with evaluation set labels. Doing so leaks information about the location of the evaluation segments and removes likely false positives from the evaluation. We cannot compare directly against this undescribed method, but provide their numbers in Table 4 for reference. Despite our more challenging evaluation procedure, we match the EP-baselineIII results and are within 2% mAP avg on 50/50 splits and nearly match performance on 75/25 splits of the EP-full model.

Detector→Classifier	ActivityNet				Thumos		
	75/25 Splits		50/50 Splits	fully-supervised	75/25 Splits	50/50 Splits	fully-supervised
	mAP@avg (n=12)	Smart	mAP@avg (n=4)	mAP@avg	mAP@avg (n=12)	mAP@avg (n=4)	mAP@avg
Clip b/32→Clip b/32	19.4 ± 0.4	22.6	17.3 ± 0.6	21.5	12.0 ± 1.4	8.0 ± 1.8	26.6
Clip b/16→Clip b/16	21.4 ± 0.7	23.5	19.5 ± 0.4	24.0	12.9 ± 1.3	9.1 ± 0.8	29.0
Clip l/14→Clip l/14	24.6 ± 0.4	28.7	22.4 ± 0.7	26.1	15.8 ± 1.6	10.5 ± 1.9	32.6
Align→Align	24.2 ± 0.7	28.1	22.9 ± 1.1	25.9	8.7 ± 1.5	6.5 ± 1.4	32.7
Basic→Basic	28.4 ± 0.5	31.2	26.4 ± 0.9	29.4	20.8 ± 2.3	16.5 ± 2.7	45.4
I3D→Clip b/32	20.2 ± 0.4	23.9	18.2 ± 0.6		14.1 ± 1.7	11.5 ± 2.6	
I3D→Clip b/16	22.1 ± 0.5	24.1	20.1 ± 0.5		15.6 ± 1.9	12.9 ± 3.1	
I3D→Clip l/14	24.8 ± 0.5	28.1	22.8 ± 0.6		17.0 ± 1.7	14.5 ± 3.2	
I3D→Align	24.8 ± 0.6	28.4	22.9 ± 1.0		10.4 ± 1.5	8.3 ± 2.1	
I3D→Basic	28.2 ± 0.5	31.3	26.4 ± 0.7		22.9 ± 2.1	19.5 ± 4.6	
EP-baselineIII [19]	20.2		16		18.8 *	15.7 *	
EP-full model [19]	23.1		19.6		23.3 *	21.9 *	

Table 4: Open-Vocabulary Temporal Action Detection. Evaluation when using a detector on one set of features and classifying those segments with the classifier to the →. On ActivityNet, mAP@Avg is mAP@0.5:0.05:0.95. On Thumos, mAP@avg is mAP@0.3:0.1:0.7. The * on the bottom rows indicates evaluations where the test set videos were trimmed to evaluation classes only. See supplemental for additional metrics.

4.7 What’s Missing from Image-Text Co-Embedding Features?

We study what information is missing from ITCE features by determining which features improve open-vocabulary TAD performance when concatenated with the ITCE features. In the supplemental, we present a large number of feature combinations on both class-agnostic and open-vocabulary detection, and only present the most synergistic combination in Table 5. Ensembling I3D_RGB + I3D_FLOW + VGGISH features with BASIC features is able to

ActivityNet - 75/25 split average (n=12)

Features	CLIP-b/32	CLIP-b/16	CLIP-l/14	ALIGN	BASIC	avg. diff.
B	19.4 ± 0.4	21.4 ± 0.7	24.6 ± 0.4	24.2 ± 0.7	28.4 ± 0.5	N/A
B+F	20 ± 1	22.1 ± 0.9	24.8 ± 0.9	25.3 ± 1.3	28.6 ± 1	0.935
B+F+A	20 ± 1	22 ± 0.9	24.8 ± 0.9	25.3 ± 1.4	28.3 ± 1	0.887
B+F+A+V	20.2 ± 1	22.4 ± 1.1	25.1 ± 0.8	25.3 ± 1.3	28.8 ± 0.9	1.130

ActivityNet - Smart split

B	22.6	23.5	25.7	26.9	29.5	N/A
B+F	23.5	23.9	27.2	28.7	32.2	1.5
B+F+A	24.3	24.6	28.6	29.4	32.0	2.2
B+F+A+V	23.8	24.4	28.2	29.3	32.1	1.9

Thumos - 75/25 split average (n=12)

B	12 ± 1.4	12.9 ± 1.3	15.8 ± 1.6	8.7 ± 1.5	20.8 ± 2.3	N/A
B+F	11.5 ± 3.3	12.8 ± 2.4	17.7 ± 2.4	9.4 ± 2.5	18.9 ± 4.6	0.102
B+F+A	12.7 ± 3.1	14.9 ± 3.6	18.6 ± 2.6	7.2 ± 2.2	20.1 ± 4.2	0.769
B+F+A+V	13.9 ± 3.2	16 ± 4	16.9 ± 3	10.4 ± 3	21.1 ± 4.3	1.725

Table 5: Open Vocabulary Detection with Ensembled Detection Features. The benefits of ensembling synergistic features for open-vocabulary detection: B - the base ITCE feature alone; B+F - adding I3D_FLOW; B+F+A - also adding VGGISH audio; B+F+A+V - also adding I3D_RGB video features. ActivityNet split average is mAP@0.5:0.05:0.95. Thumos split average is mAP@0.3:0.1:0.7. See supplemental for additional metrics.

Open vocabulary					Supervised, self-contained			Supervised, ensemble		
EP-full [19]		Ours (best)			P-GCN	PCG-TAL	TadTR	AFSD	Action Former[50]	TadTR
75/25	50/50	75/25	50/50	Smart	[49]	[37]	[24]	[22]		[24]
23.1	19.6	28.8	26.4	32.2	27.0	27.34	33.85	34.39	36.0	36.8

Table 6: State-of-the-art comparison on ActivityNet across different methods. Numbers are mAP@0.5:0.05:0.95 performance on ActivityNet. “Supervised, Self-contained” methods may use pretraining and train on ActivityNet TAD, but do not use auxiliary classifiers trained on ActivityNet video classification which “Supervised, ensemble” methods do.

boost models above 32% Avg AP@0.5:0.05:0.95 on the Smart split of ActivityNet. Across the board we often seem 1-2% mAP avg improvements when ensembling features, although results on Thumos are noisy. These particular features capture complementary information about short-term dynamics (e.g. I3D_FLOW) or different modalities (e.g. VGGISH). The feature that produced the largest, reliable boost is I3D_FLOW.

4.8 Comparison of Open-vocabulary Methods to State of the Art

We compare our model against those in the literature in Table 6 with further comparisons in the supplemental. Ensembling BASIC features with I3D RGB+FLOW and Yamnet audio features results in impressive open-vocabulary performance of 28.8% mAP avg on the random 75/25 splits and 32.2% mAP avg on the Smart split. This performance compares well to self-contained fully-supervised models in the literature that do not use dedicated ActivityNet video classification models. It outperforms models from a year ago [37, 49] and approaches the performance of concurrent work [24]. Our model still trails ensemble models that use dedicated ActivityNet video classification models [22, 24, 50], but are much closer than other open-vocabulary work [19].

5 Conclusion

In conclusion, we show that ITCEs applied to open-vocabulary temporal action detection are very powerful and almost match the performance of fully supervised models of similar complexity. These features can be complemented by adding flow and audio based features that capture information about short-term dynamics or different modalities. Due to its high performance and relative simplicity, our approach proves the potential of open-vocabulary TAD to supplant fully-supervised methods, extending the capabilities of video action detection models to classes of events and users not well represented by existing fully-supervised datasets. From this basis, we hope future work will extend our straightforward open-vocabulary temporal action detection with models that incorporate more task-specific elements, such as prompt-engineering or bottom-up boundary prediction, and we hope for a broader range of data sets that define segment boundaries in consistent, meaningful ways.

References

- [1] Humam Alwassel, Fabian Caba Heilbron, Victor Escorcia, and Bernard Ghanem. Diagnosing error in temporal action detectors. In *The European Conference on Computer Vision (ECCV)*, September 2018.
- [2] Humam Alwassel, Silvio Giancola, and Bernard Ghanem. TSP: Temporally-Sensitive Pretraining of Video Encoders for Localization Tasks. In *Proceedings of the IEEE/CVF International Conference on Computer Vision (ICCV) Workshops*, 2021.
- [3] Anurag Arnab, Mostafa Dehghani, Georg Heigold, Chen Sun, Mario Lučić, and Cordelia Schmid. Vivit: A video vision transformer. In *Proceedings of the IEEE/CVF International Conference on Computer Vision*, pages 6836–6846, 2021.
- [4] Jimmy Lei Ba, Jamie Ryan Kiros, and Geoffrey E Hinton. Layer normalization. *arXiv preprint arXiv:1607.06450*, 2016.
- [5] Ankan Bansal, Karan Sikka, Gaurav Sharma, Rama Chellappa, and Ajay Divakaran. Zero-shot object detection. In *Proceedings of the European Conference on Computer Vision (ECCV)*, pages 384–400, 2018.
- [6] Nicolas Carion, Francisco Massa, Gabriel Synnaeve, Nicolas Usunier, Alexander Kirillov, and Sergey Zagoruyko. End-to-end object detection with transformers. In Andrea Vedaldi, Horst Bischof, Thomas Brox, and Jan-Michael Frahm, editors, *Computer Vision - ECCV 2020 - 16th European Conference, Glasgow, UK, August 23-28, 2020, Proceedings, Part I*, volume 12346 of *Lecture Notes in Computer Science*, pages 213–229. Springer, 2020. doi: 10.1007/978-3-030-58452-8_13. URL https://doi.org/10.1007/978-3-030-58452-8_13.
- [7] Joao Carreira and Andrew Zisserman. Quo vadis, action recognition? a new model and the kinetics dataset. In *Proceedings of the IEEE Conference on Computer Vision and Pattern Recognition (CVPR)*, July 2017.
- [8] Yu-Wei Chao, Sudheendra Vijayanarasimhan, Bryan Seybold, David A. Ross, Jia Deng, and Rahul Sukthankar. Rethinking the faster R-CNN architecture for temporal action localization. In *Proceedings of the IEEE Conference on Computer Vision and Pattern Recognition*, 2018.
- [9] Jia Deng, Wei Dong, Richard Socher, Li-Jia Li, Kai Li, and Li Fei-Fei. Imagenet: A large-scale hierarchical image database. In *2009 IEEE conference on computer vision and pattern recognition*, pages 248–255. Ieee, 2009.
- [10] Kaiwen Duan, Song Bai, Lingxi Xie, Honggang Qi, Qingming Huang, and Qi Tian. Centernet: Keypoint triplets for object detection, 2019. URL <http://arxiv.org/abs/1904.08189>. cite arxiv:1904.08189Comment: 10 pages (including 2 pages of References), 7 figures, 5 tables.
- [11] Bernard Ghanem Fabian Caba Heilbron, Victor Escorcia and Juan Carlos Nieves. Activitynet: A large-scale video benchmark for human activity understanding. In *Proceedings of the IEEE Conference on Computer Vision and Pattern Recognition*, pages 961–970, 2015.

- [12] Jort F. Gemmeke, Daniel P. W. Ellis, Dylan Freedman, Aren Jansen, Wade Lawrence, R. Channing Moore, Manoj Plakal, and Marvin Ritter. Audio set: An ontology and human-labeled dataset for audio events. In *2017 IEEE International Conference on Acoustics, Speech and Signal Processing (ICASSP)*, pages 776–780, 2017. doi: 10.1109/ICASSP.2017.7952261.
- [13] Xiuye Gu, Tsung-Yi Lin, Weicheng Kuo, and Yin Cui. Zero-shot detection via vision and language knowledge distillation. *CoRR*, abs/2104.13921, 2021. URL <https://arxiv.org/abs/2104.13921>.
- [14] Shawn Hershey, Sourish Chaudhuri, Daniel P. W. Ellis, Jort F. Gemmeke, Aren Jansen, Channing Moore, Manoj Plakal, Devin Platt, Rif A. Saurous, Bryan Seybold, Malcolm Slaney, Ron Weiss, and Kevin Wilson. Cnn architectures for large-scale audio classification. In *International Conference on Acoustics, Speech and Signal Processing (ICASSP)*, 2017. URL <https://arxiv.org/abs/1609.09430>.
- [15] Jonathan Huang, Vivek Rathod, Chen Sun, Menglong Zhu, Anoop Korattikara, Alireza Fathi, Ian Fischer, Zbigniew Wojna, Yang Song, Sergio Guadarrama, et al. Speed/accuracy trade-offs for modern convolutional object detectors. In *Proceedings of the IEEE conference on computer vision and pattern recognition*, pages 7310–7311, 2017.
- [16] Haroon Idrees, Amir Roshan Zamir, Yu-Gang Jiang, Alex Gorban, Ivan Laptev, Rahul Sukthankar, and Mubarak Shah. The THUMOS challenge on action recognition for videos "in the wild". *CoRR*, abs/1604.06182, 2016. URL <http://arxiv.org/abs/1604.06182>.
- [17] Ashraf Islam and Richard Radke. Weakly supervised temporal action localization using deep metric learning. In *Proceedings of the IEEE/CVF Winter Conference on Applications of Computer Vision*, pages 547–556, 2020.
- [18] Chao Jia, Yinfei Yang, Ye Xia, Yi-Ting Chen, Zarana Parekh, Hieu Pham, Quoc Le, Yun-Hsuan Sung, Zhen Li, and Tom Duerig. Scaling up visual and vision-language representation learning with noisy text supervision. In *International Conference on Machine Learning*, pages 4904–4916. PMLR, 2021.
- [19] Chen Ju, Tengda Han, Kunhao Zheng, Ya Zhang, and Weidi Xie. Prompting visual-language models for efficient video understanding. In *European Conference on Computer Vision (ECCV)*. Springer, 2022.
- [20] Will Kay, João Carreira, Karen Simonyan, Brian Zhang, Chloe Hillier, Sudheendra Vijayanarasimhan, Fabio Viola, Tim Green, Trevor Back, Paul Natsev, Mustafa Suleyman, and Andrew Zisserman. The kinetics human action video dataset. *CoRR*, abs/1705.06950, 2017. URL <http://arxiv.org/abs/1705.06950>.
- [21] Zhihui Li, Lina Yao, Xiaoqin Zhang, Xianzhi Wang, Salil S. Kanhere, and Huaxiang Zhang. Zero-shot object detection with textual descriptions. In *The Thirty-Third AAAI Conference on Artificial Intelligence, AAAI 2019, The Thirty-First Innovative Applications of Artificial Intelligence Conference, IAAI 2019, The Ninth AAAI Symposium on Educational Advances in Artificial Intelligence, EAAI 2019, Honolulu, Hawaii, USA, January 27 - February 1, 2019*, pages 8690–8697. AAAI Press, 2019.

- doi: 10.1609/aaai.v33i01.33018690. URL <https://doi.org/10.1609/aaai.v33i01.33018690>.
- [22] Chuming Lin, Chengming Xu, Donghao Luo, Yabiao Wang, Ying Tai, Chengjie Wang, Jilin Li, Feiyue Huang, and Yanwei Fu. Learning salient boundary feature for anchor-free temporal action localization. In *Proceedings of the IEEE/CVF Conference on Computer Vision and Pattern Recognition*, pages 3320–3329, 2021.
- [23] Tianwei Lin, Xiao Liu, Xin Li, Errui Ding, and Shilei Wen. BMN: boundary-matching network for temporal action proposal generation. In *2019 IEEE/CVF International Conference on Computer Vision, ICCV 2019, Seoul, Korea (South), October 27 - November 2, 2019*, pages 3888–3897. IEEE, 2019. doi: 10.1109/ICCV.2019.00399. URL <https://doi.org/10.1109/ICCV.2019.00399>.
- [24] Xiaolong Liu, Qimeng Wang, Yao Hu, Xu Tang, Song Bai, and Xiang Bai. End-to-end temporal action detection with transformer, 2021.
- [25] Huaishao Luo, Lei Ji, Ming Zhong, Yang Chen, Wen Lei, Nan Duan, and Tianrui Li. Clip4clip: An empirical study of CLIP for end to end video clip retrieval. *CoRR*, abs/2104.08860, 2021. URL <https://arxiv.org/abs/2104.08860>.
- [26] Arsha Nagrani, Shan Yang, Anurag Arnab, Aren Jansen, Cordelia Schmid, and Chen Sun, editors. *Attention Bottlenecks for Multimodal Fusion*, 2021.
- [27] Arsha Nagrani, Shan Yang, Anurag Arnab, Aren Jansen, Cordelia Schmid, and Chen Sun. Attention bottlenecks for multimodal fusion. *Advances in Neural Information Processing Systems*, 34, 2021.
- [28] Arsha Nagrani, Paul Hongsuck Seo, Bryan Seybold, Anja Hauth, Santiago Manen, Chen Sun, and Cordelia Schmid. Learning audio-video modalities from image captions. *arXiv preprint arXiv:2204.00679*, 2022.
- [29] Sanath Narayan, Hisham Cholakkal, Munawar Hayat, Fahad Shahbaz Khan, Ming-Hsuan Yang, and Ling Shao. D2-net: Weakly-supervised action localization via discriminative embeddings and denoised activations. In *Proceedings of the IEEE/CVF International Conference on Computer Vision*, pages 13608–13617, 2021.
- [30] Alejandro Newell, Kaiyu Yang, and Jia Deng. Stacked hourglass networks for human pose estimation. In *European conference on computer vision*, pages 483–499. Springer, 2016.
- [31] Hieu Pham, Zihang Dai, Golnaz Ghiasi, Hanxiao Liu, Adams Wei Yu, Minh-Thang Luong, Mingxing Tan, and Quoc V. Le. Combined scaling for zero-shot transfer learning. *CoRR*, abs/2111.10050, 2021. URL <https://arxiv.org/abs/2111.10050>.
- [32] Alec Radford, Jong Wook Kim, Chris Hallacy, Aditya Ramesh, Gabriel Goh, Sandhini Agarwal, Girish Sastry, Amanda Askell, Pamela Mishkin, Jack Clark, Gretchen Krueger, and Ilya Sutskever. Learning transferable visual models from natural language supervision. In Marina Meila and Tong Zhang, editors, *Proceedings of the 38th International Conference on Machine Learning, ICML 2021, 18-24 July 2021, Virtual Event*, volume 139 of *Proceedings of Machine Learning Research*, pages 8748–8763. PMLR, 2021. URL <http://proceedings.mlr.press/v139/radford21a.html>.

- [33] Shafin Rahman, Salman Khan, and Nick Barnes. Improved visual-semantic alignment for zero-shot object detection. *34th AAAI Conference on Artificial Intelligence*, 2020.
- [34] Olaf Ronneberger, Philipp Fischer, and Thomas Brox. U-net: Convolutional networks for biomedical image segmentation. In *International Conference on Medical image computing and computer-assisted intervention*, pages 234–241. Springer, 2015.
- [35] Zheng Shou, Jonathan Chan, Alireza Zareian, Kazuyuki Miyazawa, and Shih-Fu Chang. Cdc: Convolutional-de-convolutional networks for precise temporal action localization in untrimmed videos. In *CVPR*, 2017.
- [36] Jonathan C. Stroud, David A. Ross, Chen Sun, Jia Deng, Rahul Sukthankar, and Cordelia Schmid. Learning video representations from textual web supervision. *CoRR*, abs/2007.14937, 2020. URL <https://arxiv.org/abs/2007.14937>.
- [37] Rui Su, Dong Xu, Lu Sheng, and Wanli Ouyang. Pcg-tal: Progressive cross-granularity cooperation for temporal action localization. *IEEE Transactions on Image Processing*, 30:2103–2113, 2020.
- [38] Chen Sun, Abhinav Shrivastava, Saurabh Singh, and Abhinav Gupta. Revisiting Unreasonable Effectiveness of Data in Deep Learning Era. In *IEEE International Conference on Computer Vision (ICCV)*, 2017.
- [39] Tensorflow. Models/research/audioset/yamnet at master · tensorflow/models, 2020. URL <https://github.com/tensorflow/models/tree/master/research/audioset/yamnet>.
- [40] Limin Wang, Yuanjun Xiong, Dahua Lin, and Luc Van Gool. Untrimmednets for weakly supervised action recognition and detection. In *Proceedings of the IEEE conference on Computer Vision and Pattern Recognition*, pages 4325–4334, 2017.
- [41] Mengmeng Wang, Jiazheng Xing, and Yong Liu. Actionclip: A new paradigm for video action recognition. *CoRR*, abs/2109.08472, 2021. URL <https://arxiv.org/abs/2109.08472>.
- [42] Qiang Wang, Yanhao Zhang, Yun Zheng, and Pan Pan. Rcl: Recurrent continuous localization for temporal action detection. In *2022 IEEE/CVF Conference on Computer Vision and Pattern Recognition (CVPR)*, pages 13556–13565, 2022. doi: 10.1109/CVPR52688.2022.01320.
- [43] Yu Kong Wentao Bao, Qi Yu. Opental: Towards open set temporal action localization. In *Proceedings of the IEEE/CVF Conference on Computer Vision and Pattern Recognition (CVPR)*, June 2022.
- [44] Yuanjun Xiong, Limin Wang, Zhe Wang, Bowen Zhang, Hang Song, Wei Li, Dahua Lin, Yu Qiao, Luc Van Gool, and Xiaoou Tang. CUHK & ETHZ & SIAT submission to activitynet challenge 2016. *CoRR*, abs/1608.00797, 2016. URL <http://arxiv.org/abs/1608.00797>.
- [45] Huijuan Xu, Abir Das, and Kate Saenko. R-c3d: region convolutional 3d network for temporal activity detection. In *ICCV*, pages 5794–5803, 2017.

- [46] Mengmeng Xu, Chen Zhao, David S. Rojas, Ali K. Thabet, and Bernard Ghanem. G-TAD: sub-graph localization for temporal action detection. In *2020 IEEE/CVF Conference on Computer Vision and Pattern Recognition, CVPR 2020, Seattle, WA, USA, June 13-19, 2020*, pages 10153–10162. Computer Vision Foundation / IEEE, 2020. doi: 10.1109/CVPR42600.2020.01017. URL https://openaccess.thecvf.com/content_CVPR_2020/html/Xu_G-TAD_Sub-Graph_Localization_for_Temporal_Action_Detection_CVPR_2020_paper.html.
- [47] Le Yang, Houwen Peng, Dingwen Zhang, Jianlong Fu, and Junwei Han. Revisiting anchor mechanisms for temporal action localization. *IEEE Transactions on Image Processing*, 29:8535–8548, 2020.
- [48] Alireza Zareian, Kevin Dela Rosa, Derek Hao Hu, and Shih-Fu Chang. Open-vocabulary object detection using captions. In *Proceedings of the IEEE/CVF Conference on Computer Vision and Pattern Recognition*, pages 14393–14402, 2021.
- [49] Runhao Zeng, Wenbing Huang, Mingkui Tan, Yu Rong, Peilin Zhao, Junzhou Huang, and Chuang Gan. Graph convolutional networks for temporal action localization. In *The IEEE International Conference on Computer Vision (ICCV)*, October 2019.
- [50] Chenlin Zhang, Jianxin Wu, and Yin Li. Actionformer: Localizing moments of actions with transformers, 2022.
- [51] Peisen Zhao, Lingxi Xie, Chen Ju, Ya Zhang, Yanfeng Wang, and Qi Tian. Bottom-up temporal action localization with mutual regularization. In *ECCV*, 2020.
- [52] Yue Zhao, Yuanjun Xiong, Limin Wang, Zhirong Wu, Xiaoou Tang, and Dahua Lin. Temporal action detection with structured segment networks. *Int. J. Comput. Vis.*, 128(1):74–95, 2020. doi: 10.1007/s11263-019-01211-2. URL <https://doi.org/10.1007/s11263-019-01211-2>.
- [53] Pengkai Zhu, Hanxiao Wang, and Venkatesh Saligrama. Don’t even look once: Synthesizing features for zero-shot detection. In *2020 IEEE/CVF Conference on Computer Vision and Pattern Recognition, CVPR 2020, Seattle, WA, USA, June 13-19, 2020*, pages 11690–11699, 2020. doi: 10.1109/CVPR42600.2020.01171. URL https://openaccess.thecvf.com/content_CVPR_2020/html/Zhu_Dont_Even_Look_Once_Synthesizing_Features_for_Zero-Shot_Detection_CVPR_2020_paper.html.

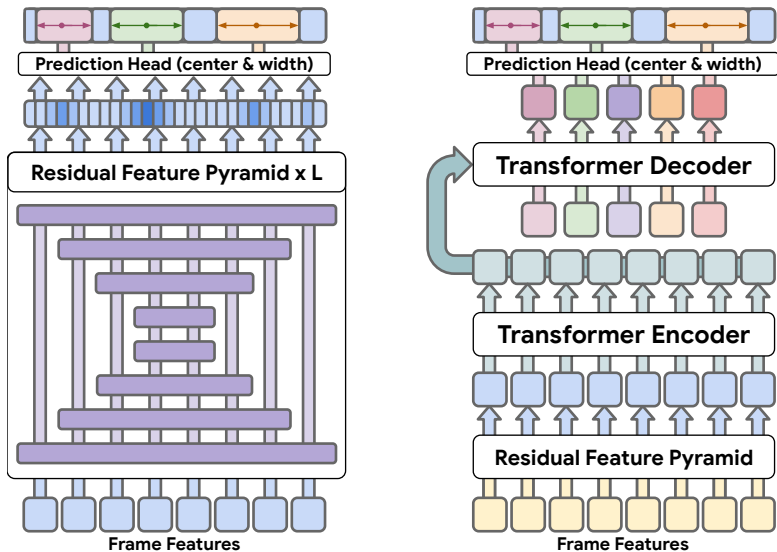


Figure 2: Class-Agnostic detection architectures used in our experiments. (Left) Illustration of the CenterNet[10] based class-agnostic detector, which applies a residual feature pyramid (RFP) followed by action prediction heads. (Right) Illustration of the DETR[6] based model, which first applies RFP to input features followed by transformer encoder and decoder layers. See text for details.

A Class-Agnostic Detection Architectures

Figure 2 is an overview of our class-agnostic detection architectures that we describe in detail below.

A.1 Residual Feature Pyramid

We construct a residual feature pyramid inspired by [30] to mix temporal information and generate appropriate inputs for detection heads. We construct and stack multiple U-Net[34]-style architectures on top of one another. We use residual connections extensively throughout the network and across stacked towers at the same resolution. We call our particular configuration a Residual Feature Pyramid (RFP).

Supplemental Figure 3 details one resolution of the RFP in the descending then ascending directions. Inputs for this resolution come in from downsampling the higher resolution and features at the same resolution from previous RFPs in the stack. The input features are summed and passed to two residual blocks. After two blocks the features are downsampled via a strided convolution and passed to a similar, nested processing stage at a lower resolution. The upsampled outputs of the lower resolution are summed with the previous residual values and passed to two more residual blocks. The final output is then upsampled via strided transposed convolution and processed by the higher resolution. Our residual blocks are a 0) Input storage, 1) ReLU activation, 2) Convolution, 3) LayerNormalization, 4) ReLU activation, 5) Convolution, 6) LayerNormalization, and 7) Residual addition to the stored input. If downsampling or upsampling, (5) is a stride 2 convolution or transposed convolution and the

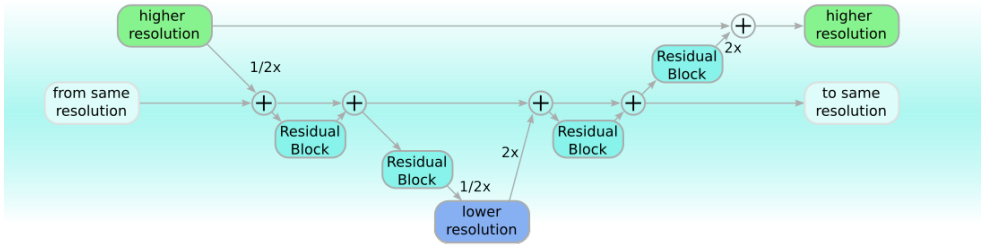


Figure 3: Diagram of one resolution in a Residual Feature Pyramid. The shaded, middle portion of diagram is at a single resolution. The top is a higher resolution, and the bottom is lower resolution. Information travels from left to right and this covers both the descending in resolution and ascending portions. Each \oplus represents a residual addition.

residual inputs (7) are processed by an additional strided convolution to match the resolution and number of dimensions.

The hyperparameters for our stacked RFP are as follows. We stack 4 descending and ascending RFPs on top of each other. Each RFP has 5 resolutions. At the highest, full resolution each convolution has 512 units. All lower resolutions use 128 units. Each kernel has a window size of 5.

A.2 DETR

We adapt the DETR[6] architecture proposed for object detection to temporal action detection (TAD) by treating TAD as a 1-d version of object detection. The DETR model consists of a transformer encoder and a decoder and treats object detection as a set prediction problem. The model takes as input a fixed number of learned object query vectors and uses prediction heads on top of the transformer outputs to predict bounding boxes and object classification scores directly.

In our adaptation, we predict segment start and end indices and action classification scores from the transformer decoder’s output with the following modifications. (1) We use a residual feature pyramid architecture to extract features, (2) we perform SOI (Segment of Interest) pooling as defined in[8] using the predicted segments and concatenate the pooled features with the transformer output before classifying the action, (3) we use learned positional encodings and perform hungarian matching on a combination of the L1 distance and IOU scores as done in [24].

Hyperparameters. We use 2 hidden layers for both the encoder and decoder, hidden size of 1024 and 16 attention heads. The prediction head consists of 2 linear layers of hidden size 1024. We set the number of segment queries to 64 and perform NMS to obtain the final set of segment detections.

A.3 CenterNet

We adapt the CenterNet[10] architecture proposed for object detection to temporal action detection (TAD) by treating TAD as a 1-d version of object detection. CenterNet produces three outputs at every input point: a logit distribution for each class label, a width if any

Model	mAP@0.5	mAP@0.75	mAP@0.95	mAP@avg	AR@10	AR@50	AR@100
Clip b/32 - our splits	48.4 ± 0.6	25.7 ± 0.7	3.3 ± 0.3	27.2 ± 0.5	41.2 ± 0.5	47.9 ± 0.4	47.9 ± 0.4
Clip b/32 - [19] splits	48.7 ± 1.0	25.7 ± 0.7	3.4 ± 0.3	27.3 ± 0.7	41.2 ± 0.6	47.2 ± 0.6	47.2 ± 0.6
Clip b/16 - our splits	49.0 ± 0.8	26.1 ± 0.6	3.2 ± 0.3	27.6 ± 0.5	42.2 ± 0.6	49.1 ± 0.7	49.1 ± 0.7
Clip b/16 - [19] splits	49.1 ± 1.0	26.2 ± 0.8	3.5 ± 0.3	27.7 ± 0.7	41.6 ± 0.5	48.4 ± 0.5	48.4 ± 0.5
Clip l/14 - our splits	49.6 ± 0.6	26.7 ± 0.5	3.8 ± 0.3	28.3 ± 0.4	42.4 ± 0.4	48.3 ± 0.5	48.3 ± 0.5
Clip l/14 - [19] splits	50.2 ± 1.0	26.7 ± 0.8	3.6 ± 0.3	28.4 ± 0.8	42.2 ± 0.6	48.3 ± 0.7	48.3 ± 0.7
Align - our splits	49.1 ± 0.6	26.4 ± 0.5	3.4 ± 0.3	27.8 ± 0.5	42.2 ± 0.4	47.8 ± 0.5	47.8 ± 0.5
Align - [19] splits	49.8 ± 1.0	26.3 ± 0.8	3.8 ± 0.4	28.0 ± 0.8	42.0 ± 0.6	47.4 ± 0.5	47.4 ± 0.5
Basic - our splits	50.3 ± 0.7	27.5 ± 0.6	3.3 ± 0.3	28.8 ± 0.5	43.3 ± 0.5	49.6 ± 0.3	49.6 ± 0.3
Basic - [19] splits	51.6 ± 0.9	27.8 ± 0.8	3.4 ± 0.2	29.3 ± 0.7	43.5 ± 0.6	48.9 ± 0.5	48.9 ± 0.5

Table 7: ActivityNet Class-Agnostic Detection Results comparing our splits to [19]. Performance of class-agnostic detectors with different input features. mAP@0.5IoUs is the mean Average Precision at 0.5 Intersection over Union. mAP@avg is the average of mAP@0.50:0.05:0.95. AR@10 is Average Recall at 10. Aggregates are means ± standard error across splits.

segment starts at that point, and an offset that shifts the center location slightly if needed. Each prediction is produced by a 2-layer convolutional network with 256 units on top of an RFP feature extractor. As in [10], we predict segments at the full resolution between stacked RFP and apply auxiliary losses at each resolution during training. During inference we only use segments from the last RFP stack. The loss for the width and offset are absolute error. The loss for the classification logits is the penalty reduced focal loss described in [10]. We weight the width by 0.1 relative to the other losses.

B Additional Results

B.1 Class-Agnostic Detection

B.1.1 Our random splits are statistically similar to [19]

[19] uses 10 random splits, and we use a different set of 12 random splits for 75/25 and 4 for 50/50. To show that our splits are statistically similar those in [19], we compare the means and standard errors on class-agnostic detection on ActivityNet with both sets of 75/25 splits in Table 7. As expected, we find that the means are often within one standard error of each other for nearly every possible comparison.

B.1.2 Variability on Thumos

Evaluation performance on Thumos moves in large, discrete jumps as shown in Supplementary Figure 4. This examples shows one evaluation curve for mAP@0.5 IoU, but the dominant behavior of large, discrete jumps in evaluation performance is consistent across many runs and all mAP metrics. This discrete behavior is because here are only five classes in the 75/25 splits of Thumos and when the class-agnostic model learns or unlearns segments applicable to that class, performance jumps. The large jumps are related to the standard error of the mean mAP being ten times as large on Thumos as on ActivityNet.

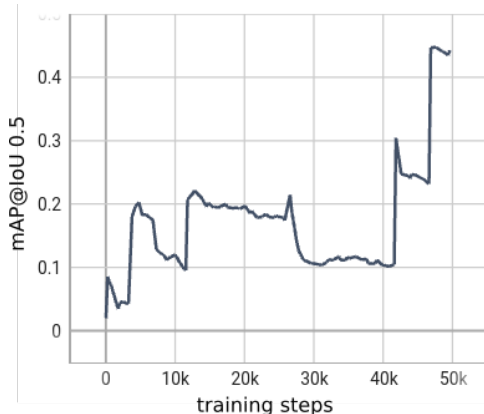


Figure 4: mAP@0.5 IoU evaluation performance on Thumos moves in large, discrete jumps.

Model	Supervised (200 class)		75/25 splits average (n=12)		Intermediate split		Smart split		50/50 splits average (n=4)	
	mAP@avg	AR@10	AP@avg	AR@10	AP@avg	AR@10	AP@avg	AR@10	AP@avg	AR@10
CLIP b/32	21.5	43.2	27.2 ± 1.0	41.3 ± 0.9	28.4	42.1	29.2	43.0	25.6 ± 0.4	38.6 ± 0.9
CLIP b/16	24.0	44.5	27.6 ± 1.0	42.4 ± 1.2	27.9	41.2	30.7	44.0	25.8 ± 0.7	40.0 ± 1.3
CLIP l/14	26.1	44.3	28.2 ± 0.8	42.5 ± 0.9	28.7	43.2	31.3	43.4	26.6 ± 0.6	40.1 ± 0.7
ALIGN	25.9	43.3	27.8 ± 0.9	42.3 ± 0.8	28.7	41.9	30.3	43.0	26.1 ± 0.9	40.1 ± 1.0
BASIC	29.4	45.7	28.8 ± 0.9	43.3 ± 0.8	28.6	43.0	32.0	44.9	27.0 ± 0.8	41.0 ± 1.1
I3D RGB+FLOW	22.6	44.6	28.4 ± 0.9	42.3 ± 0.8	28.8	44.2	30.4	43.1	26.5 ± 0.5	40.4 ± 0.7
I3D RGB	21.0	43.6	27.2 ± 0.7	41.3 ± 0.7	27.5	41.4	30.7	43.8	25.1 ± 0.3	38.9 ± 0.3
I3D FLOW	17.7	44.6	28.3 ± 1.0	42.2 ± 1.0	28.8	40.9	29.6	42.5	25.6 ± 0.5	40.3 ± 0.13
YAMNET	6.6	36.8	22.7 ± 0.6	36.6 ± 0.6	23.1	37.8	25.5	40.1	20.9 ± 1.0	34.9 ± 0.17
VGGISH	7.3	37.0	23.0 ± 0.8	36.9 ± 0.9	23.2	36.7	25.0	38.8	21.3 ± 0.5	35.6 ± 1.1
VIVIT	25.5	41.7	22.4 ± 0.8	37.1 ± 1.1	22.7	37.8	24.8	40.0	20.0 ± 0.4	34.2 ± 1.1
MBT-v	25.3	42.4	23.5 ± 0.7	38.5 ± 0.8	22.7	37.3	25.6	40.8	21.8 ± 0.4	36.9 ± 0.9
MBT-a	3.1	33.8	18.1 ± 0.8	34.1 ± 1.0	19.2	35.3	20.0	35.1	17.9 ± 0.3	33.6 ± 0.5

Table 8: ActivityNet Class-Agnostic Detection Results. Performance of class-agnostic detectors with different input features. mAP@avg is the average mAP over IoUs 0.5:0.05:0.95. AR@10 is Average Recall at 10. Data is grouped as columns for supervised, closed-vocabulary TAD, 75/25 random splits (n=12) (along with the Intermediate and Smart splits), and 50/50 random splits (n=4). Aggregates are means ± standard error across splits. See supplemental for additional metrics.

B.2 Fully supervised detection with video transformers relies on classification

Table 12 mirrors Table 2 in the main text but only shows ActivityNet performance and adds fully-supervised detection metrics. The most interesting comparisons are between the fully-supervised mAPs and the class-agnostic mAPs. For ITCE features, both metrics increase with model size and class-agnostic metrics are typically slightly better than fully-supervised ones. In contrast, for traditional features (I3D and audio models), the fully-supervised performance is much worse than class-agnostic performance. The opposite trend is true where recent vision transformer models [3, 26] perform well for fully-supervised detection, but relatively poorly for class-agnostic detection.

Feature	Image-text Model										Delta	
	CLIP-b/32		CLIP-b/16		CLIP-l/14		ALIGN		BASIC		Mean	Stderr (n=10)
	Int.	Smart	Int.	Smart	Int.	Smart	Int.	Smart	Int.	Smart		
[image-text alone]	28.50	29.70	29.00	30.40	28.80	31.50	28.50	29.30	29.30	31.70	N/A	N/A
i3d_flow	29.24	30.60	28.99	30.89	28.95	29.98	29.42	31.62	30.42	32.20	0.56	0.32
i3d_rgb	28.80	30.74	28.35	30.47	28.35	30.83	29.05	30.50	29.80	31.17	0.14	0.23
yamnet	28.46	30.32	28.14	30.35	29.52	31.01	28.39	32.03	29.06	32.10	0.27	0.33
vggish	28.40	29.69	29.42	31.13	29.83	31.53	29.27	30.35	29.85	31.95	0.47	0.14
i3d_flow,yamnet	29.20	31.01	29.82	31.54	28.75	31.66	28.97	30.86	30.11	32.97	0.82	0.17
i3d_flow,vggish	29.13	31.53	28.94	31.16	30.16	31.80	29.27	32.31	29.24	32.25	0.91	0.31
i3d_flow,i3d_rgb	28.63	30.84	29.30	30.57	29.93	32.09	29.51	31.35	29.54	31.88	0.69	0.21
i3d_flow,i3d_rgb,yamnet	28.63	31.49	29.43	30.88	28.63	31.80	29.84	31.07	30.03	32.19	0.73	0.23
i3d_flow,i3d_rgb,vggish	29.23	30.91	29.93	31.03	29.67	31.34	29.58	31.95	29.66	31.84	0.84	0.26

Table 9: ActivityNet Class-Agnostic Temporal Action Detection on Ensembled Features. Comparisons on Intermediate (Int.) and Smart splits of ActivityNet across different image-text embeddings (columns) and different ensemble features (rows). The rightmost columns are the mean and standard error across column values relative to the [image-text alone] row measuring the added benefit of using these ensemble features. See supplemental for additional metrics.

B.3 Feature Ensembles for Class Agnostic Detection on limited splits

To determine which feature ensembles improve performance, we began by testing combinations on a subset of splits in Table 9. The two splits are the Intermediate split, which was one of the random splits that happened to give intermediate performance, and the Smart split. After testing many combinations, we took the three most synergistic features, I3D_FLOW + I3D_RGB + VGGISH and computed how much benefit they added to different ITCE features in Table 10

ActivityNet - 75/25 split average (n=12)

Embedding	CLIP-b/32	CLIP-b/16	CLIP-l/14	ALIGN	BASIC	avg. diff.
B	27.2 ± 1	27.6 ± 1	28.2 ± 0.8	27.8 ± 0.9	28.8 ± 0.9	N/A
B+F	28.2 ± 0.5	28.4 ± 0.4	28.6 ± 0.5	29.1 ± 0.5	28.9 ± 0.5	0.7
B+F+A	28.2 ± 0.5	28.3 ± 0.4	28.8 ± 0.4	29.2 ± 0.5	28.6 ± 0.5	0.7
B+F+A+V	28.5 ± 0.6	28.9 ± 0.5	29 ± 0.5	29.1 ± 0.5	29 ± 0.5	1.0

ActivityNet - Smart

B	29.2	30.7	31.3	30.3	32.0	N/A
B+F	30.6	30.9	30.0	31.6	32.2	0.3
B+F+A	31.5	31.2	31.8	32.3	32.2	1.1
B+F+A+V	30.9	31.0	31.3	32.0	31.8	0.7

Thumos

B	32.2 ± 7.7	32.1 ± 8	34.8 ± 7.9	31.7 ± 7.9	33.7 ± 7.9	N/A
B+F	27.6 ± 3.8	33.2 ± 4.9	39.7 ± 3.6	38.4 ± 2.9	33.4 ± 4.2	1.1
B+F+A	30.8 ± 4.4	35.8 ± 3.7	40.5 ± 3.9	30.4 ± 4.6	28.8 ± 4.1	-0.1
B+F+A+V	35.1 ± 4.1	40.8 ± 3.7	33.8 ± 3.3	38.9 ± 2.9	36.2 ± 3.5	3.6

Table 10: Class-agnostic Detection with Feature Ensembles. The benefits of ensembling the best features from Table 9 for class-agnostic detection: B - the base image-text feature alone; B+F - adding I3D_FLOW; B+F+A - adding VGGISH audio; B+F+A+V - adding I3D_RGB video features. ActivityNet split average is mAP@0.5:0.05:0.95. Thumos split average is mAP@0.3:0.1:0.7. See supplemental for additional metrics.

Method	mAP@0.5	mAP@0.75	mAP@0.95	mAP@avg
<i>Open-Vocabulary methods</i>				
EP-full [19] - 75/25 split	37.6	22.9	3.8	23.1
Ours (best) - 75/25 split	46.6±0.5	28.4±0.6	-	28.8±0.5
EP-full [19] - 50/50 split	32.0	19.3	2.9	19.6
Ours (best) - 50/50 split	45.3±0.5	27.0±0.7	-	27.6±0.5
Ours (best) - Smart split	51.6	31.3	-	32.1
<i>Self-contained methods</i>				
CDC [35]	43.83	25.88	0.21	22.77
R-C3D [45]	26.80	-	-	-
SSN [52]	39.12	23.48	5.49	23.98
TAL-Net [8]	38.23	18.30	1.30	20.22
P-GCN [49]	42.90	28.14	2.47	26.99
TadTR [24]	40.85	28.44	7.84	27.75
<i>Combined with an ensemble of action classifiers [44]</i>				
P-GCN [49]	48.26	33.16	3.27	31.11
MR [51]	43.47	33.91	9.21	30.12
A2Net [47]	43.55	28.69	3.70	27.75
BMN [23]	50.07	34.78	8.29	33.85
G-TAD [46]	50.36	34.60	9.02	34.09
TadTR+ensemble [24]	49.08	32.58	8.49	32.27
TadTR+BMN [24]	50.51	35.35	8.18	34.55

Table 11: Comparison of different methods on ActivityNet-1.3. Methods in the first group are open-vocabulary methods, those in the second group are self-contained methods trained in the traditional supervised setting, and the third group are supervised methods combined with an ensemble of action classifiers [44].

C Open Vocabulary Detection

C.1 Expanded Comparison of Open Vocabulary Detection to State of the Art.

We present a comparison of our proposed open-vocabulary detection method to other state-of-the-art methods on ActivityNet-1.3 in table 11. In addition to a comparison against the concurrent open-vocabulary method EfficientPrompt [19], we also present results of recent fully supervised action detection methods, including methods which utilize an ensemble of action classifiers. We observe that our method significantly outperforms in the open-vocabulary setting. Our approach is even competitive with state-of-the-art fully-supervised self-contained methods with random splits and outperforms them by a large amount on the Smart split. Because the data distribution for training and testing classes matches in the fully-supervised setting, our Smart split results are the more appropriate comparison. Our results on the Smart split are event approaching ensembles of multiple action classifiers specific to the ActivityNet data set. Note, that the results presented here are from our models with the best combination of input features, and a full breakdown of results with different input feature ensembles can be found in section C.3.

C.2 MBT Video Model

We also evaluate a segment-level classification model for open vocabulary TAD using the recently proposed Multi-modal Bottleneck Transformer (MBT) [26]. MBT is a segment-level model that takes 32 video frames as input and learns segment embeddings that are close to textual descriptions of videos. The base architecture of MBT is equivalent to Clip b/32 in terms of the number of parameters. We use the WTS-70M[36] dataset which is a weakly supervised dataset containing internet video titles to train the model. Table 14 provides results using the MBT model as the open vocabulary classifier. MBT performs better than its equivalent Clip models suggesting that segment level embeddings encode more information than frame-level ones. However, it is still weaker than stronger image architectures such as Align/Basic. We plan to further explore this model with stronger architectures and additional features such as audio in the future.

C.3 Exhaustive Tables

Because we test so many combinations of features over different splits, the tables of results with all of the standard metrics were too cluttered for a readable main text. To still provide all of the standard metrics, we provide these exhaustive tables in the supplemental that add columns that were omitted in the main text and adjust the layout.

Exhaustive Table Index:

- Table 12 - ActivityNet Class-Agnostic Detection Results.
- Table 13 - Thumos Class-Agnostic Detection Results.
- Table 14 - ActivityNet Open Vocabulary Detection Results.
- Table 15 - Thumos Open Vocabulary Detection Results.
- Table 16 - ActivityNet Class-Agnostic Detection Results for Feature Ensembles on a Subset of Splits.
- Table 17 - ActivityNet Class-Agnostic Detection Results for Feature Ensembles.
- Table 18 - Thumos Class-Agnostic Detection Results for Feature Ensembles.
- Table 19 - ActivityNet Open Vocabulary Detection Results for Feature Ensembles.
- Table 20 - Thumos Open Vocabulary Detection Results for Feature Ensembles.
- Table 21 - ActivityNet Random 75/25 Splits.
- Table 22 - ActivityNet Random 50/50 Splits.
- Table 23 - Thumos Random 75/25 Splits.
- Table 24 - Thumos Random 50/50 Splits.

Model	mAP@0.5	mAP@0.75	mAP@0.95	mAP@avg	AR@10	AR@50	AR@100
Clip b/32 - 75/25	48.4 ± 0.6	25.7 ± 0.7	3.3 ± 0.3	27.2 ± 0.5	41.2 ± 0.5	47.9 ± 0.4	47.9 ± 0.4
Clip b/32 - Intermediate	49.5	26.9	4.2	28.4	42.1	49.5	49.5
Clip b/32 - Smart	50.4	27.4	4.2	29.2	42.5	50.0	50.0
Clip b/32 - 50/50	47.5 ± 0.7	24.5 ± 1.3	2.8 ± 0.7	26.2 ± 1.1	39.8 ± 0.9	47.2 ± 1.3	47.2 ± 1.3
Clip b/16 - 75/25	49.0 ± 0.8	26.1 ± 0.6	3.2 ± 0.3	27.6 ± 0.5	42.2 ± 0.6	49.1 ± 0.7	49.1 ± 0.7
Clip b/16 - Intermediate	50.1	26.0	3.9	27.9	41.2	47.6	47.6
Clip b/16 - Smart	52.0	29.1	5.1	30.7	43.9	50.4	50.4
Clip b/16 - 50/50	47.6 ± 0.6	24.6 ± 0.8	2.5 ± 0.6	26.3 ± 0.7	40.5 ± 1.5	46.8 ± 1.6	46.8 ± 1.6
Clip I/14 - 75/25	49.6 ± 0.6	26.7 ± 0.5	3.8 ± 0.3	28.3 ± 0.4	42.4 ± 0.4	48.3 ± 0.5	48.3 ± 0.5
Clip I/14 - Intermediate	49.1	27.1	4.9	28.7	43.3	49.8	49.8
Clip I/14 - Smart	53.5	29.1	5.4	31.3	44.1	48.7	48.7
Clip I/14 - 50/50	48.5 ± 0.9	24.7 ± 0.7	3.0 ± 0.5	26.6 ± 0.7	41.0 ± 1.2	47.1 ± 1.3	47.1 ± 1.3
Align - 75/25	49.1 ± 0.6	26.4 ± 0.5	3.4 ± 0.3	27.8 ± 0.5	42.2 ± 0.4	47.8 ± 0.5	47.8 ± 0.5
Align - Intermediate	50.2	27.3	4.2	28.7	41.8	46.8	46.8
Align - Smart	52.1	28.5	4.6	30.3	43.6	47.3	47.3
Align - 50/50	47.5 ± 1.5	24.1 ± 0.8	3.3 ± 0.5	26.1 ± 0.9	39.9 ± 1.0	46.0 ± 0.8	46.0 ± 0.8
Basic - 75/25	50.3 ± 0.7	27.5 ± 0.6	3.3 ± 0.3	28.8 ± 0.5	43.3 ± 0.5	49.6 ± 0.3	49.6 ± 0.3
Basic - Intermediate	50.9	26.6	3.9	28.6	43.2	49.5	49.5
Basic - Smart	54.3	30.5	5.1	32.0	45.5	50.0	50.0
Basic - 50/50	48.3 ± 0.3	25.5 ± 0.5	2.7 ± 1.2	26.8 ± 0.7	40.7 ± 1.0	47.6 ± 1.0	47.6 ± 1.0
I3D_RGB+I3D_FLOW - 75/25	50.1 ± 0.6	27.1 ± 0.6	2.8 ± 0.2	28.4 ± 0.5	42.2 ± 0.4	48.5 ± 0.4	48.5 ± 0.4
I3D_RGB+I3D_FLOW - Intermediate	50.5	27.4	3.1	28.8	44.0	50.2	50.2
I3D_RGB+I3D_FLOW - Smart	53.1	29.0	2.7	30.4	42.9	49.0	49.0
I3D_RGB+I3D_FLOW - 50/50	48.1 ± 0.6	25.0 ± 0.6	1.9 ± 0.0	26.5 ± 0.5	40.3 ± 0.7	46.5 ± 1.0	46.5 ± 1.0
I3D_RGB - 75/25	48.8 ± 0.6	25.7 ± 0.4	2.4 ± 0.2	27.2 ± 0.4	41.2 ± 0.3	47.6 ± 0.3	47.6 ± 0.3
I3D_RGB - Intermediate	49.9	25.3	3.0	27.5	41.3	47.7	47.7
I3D_RGB - Smart	51.5	28.1	3.7	29.6	42.5	49.2	49.2
I3D_RGB - 50/50	47.8 ± 1.1	24.5 ± 1.5	2.0 ± 0.5	26.2 ± 1.1	39.8 ± 1.3	46.9 ± 1.3	46.9 ± 1.3
I3D_FLOW - 75/25	49.8 ± 0.7	27.1 ± 0.6	2.7 ± 0.3	28.3 ± 0.5	42.0 ± 0.5	48.6 ± 0.6	48.6 ± 0.6
I3D_FLOW - Intermediate	51.6	27.3	2.7	28.8	41.0	46.4	46.4
I3D_FLOW - Smart	52.3	29.7	3.3	30.7	43.7	50.0	50.0
I3D_FLOW - 50/50	46.8 ± 0.8	24.9 ± 1.0	1.8 ± 0.1	26.1 ± 0.8	40.6 ± 1.0	47.3 ± 1.1	47.3 ± 1.1
YAMNET - 75/25	41.5 ± 0.5	21.5 ± 0.4	1.8 ± 0.2	22.7 ± 0.3	35.8 ± 0.3	45.9 ± 0.3	46.0 ± 0.4
YAMNET - Intermediate	42.4	22.3	1.2	23.1	36.5	47.5	47.5
YAMNET - Smart	45.0	24.4	2.3	25.5	38.4	48.4	48.7
YAMNET - 50/50	39.8 ± 0.8	19.8 ± 1.6	1.3 ± 0.3	21.3 ± 1.2	34.3 ± 1.5	44.9 ± 1.5	44.9 ± 1.5
VGGISH - 75/25	42.0 ± 0.5	21.8 ± 0.5	1.8 ± 0.2	23.0 ± 0.4	36.0 ± 0.4	46.5 ± 0.5	46.6 ± 0.5
VGGISH - Intermediate	41.6	22.6	1.6	23.2	35.7	46.2	46.2
VGGISH - Smart	45.9	23.6	2.0	25.0	39.2	48.3	48.3
VGGISH - 50/50	41.0 ± 1.3	20.2 ± 1.3	1.7 ± 0.6	21.8 ± 1.1	36.0 ± 1.4	45.4 ± 2.2	45.4 ± 2.2
VIVIT - 75/25	43.0 ± 0.7	20.6 ± 0.5	0.8 ± 0.1	22.4 ± 0.4	36.0 ± 0.5	43.7 ± 0.6	43.7 ± 0.6
VIVIT - Intermediate	42.9	21.2	1.1	22.7	36.5	43.9	43.9
VIVIT - Smart	46.2	23.0	1.3	24.8	38.8	46.9	46.9
VIVIT - 50/50	41.2 ± 0.8	18.9 ± 1.3	0.7 ± 0.2	21.0 ± 0.8	34.4 ± 1.3	42.1 ± 1.2	42.1 ± 1.2
MBT-audio - 75/25	37.7 ± 0.6	15.8 ± 0.5	0.2 ± 0.0	18.1 ± 0.4	32.7 ± 0.4	43.1 ± 0.5	43.3 ± 0.4
MBT-audio - Intermediate	38.3	17.3	0.2	19.2	34.3	42.6	42.6
MBT-audio - Smart	40.6	17.5	0.3	20.0	34.7	42.0	42.0
MBT-audio - 50/50	37.4 ± 0.7	15.3 ± 0.6	0.1 ± 0.1	17.7 ± 0.6	32.1 ± 0.6	42.8 ± 0.4	42.9 ± 0.3
MBT-video - 75/25	44.8 ± 0.6	21.4 ± 0.4	0.9 ± 0.1	23.5 ± 0.4	37.6 ± 0.4	44.1 ± 0.3	44.1 ± 0.3
MBT-video - Intermediate	43.8	20.4	0.8	22.7	36.8	43.7	43.7
MBT-video - Smart	47.7	23.9	0.9	25.6	39.6	46.5	46.5
MBT-video - 50/50	43.7 ± 0.4	19.9 ± 0.2	0.7 ± 0.2	22.3 ± 0.2	36.7 ± 0.7	43.6 ± 0.9	43.6 ± 0.9

Table 12: ActivityNet Class-Agnostic Detection Results. Performance of class-agnostic detectors with different input features. mAP@0.5IoUs is the mean Average Precision at 0.5 Intersection over Union. mAP@avg is the average of mAP@0.50:0.05:0.95. AR@10 is Average Recall at 10. Aggregates are means ± standard error across splits.

Model	mAP@0.3	mAP@0.4	mAP@0.5	mAP@0.6	mAP@0.7	mAP@avg	AR@10	AR@50	AR@100
Clip b/32 - 75/25	49.6 ± 3.9	41.3 ± 4.0	32.2 ± 4.0	23.6 ± 4.2	16.4 ± 4.0	32.6 ± 3.9	14.3 ± 1.7	28.2 ± 2.8	32.7 ± 2.7
Clip b/32 - 50/50	33.4 ± 7.9	25.7 ± 7.1	17.8 ± 6.1	10.6 ± 4.4	5.1 ± 2.4	18.5 ± 5.5	8.8 ± 3.2	20.3 ± 4.1	27.0 ± 3.9
Clip b/16 - 75/25	46.5 ± 4.1	39.6 ± 4.1	32.1 ± 4.2	24.3 ± 4.1	17.7 ± 4.0	32.0 ± 4.0	14.1 ± 1.8	29.5 ± 2.5	34.5 ± 2.5
Clip b/16 - 50/50	41.2 ± 5.8	32.0 ± 5.6	21.9 ± 4.7	12.4 ± 3.4	5.5 ± 1.8	22.6 ± 4.1	9.7 ± 1.9	21.7 ± 3.2	25.9 ± 2.9
Clip I/14 - 75/25	53.4 ± 3.5	44.4 ± 3.9	34.8 ± 4.1	25.8 ± 4.2	17.6 ± 4.0	35.2 ± 3.8	15.6 ± 1.7	28.8 ± 2.8	33.4 ± 2.8
Clip I/14 - 50/50	47.9 ± 4.6	37.0 ± 5.8	25.0 ± 5.7	14.8 ± 4.9	7.9 ± 3.7	26.5 ± 4.7	10.5 ± 2.0	21.8 ± 4.2	25.9 ± 4.3
Align - 75/25	47.3 ± 4.2	39.8 ± 4.2	31.7 ± 4.1	23.0 ± 4.0	15.8 ± 3.9	31.5 ± 3.9	14.2 ± 1.7	29.5 ± 2.3	34.5 ± 2.4
Align - 50/50	44.1 ± 3.3	33.2 ± 3.9	23.4 ± 4.7	15.7 ± 5.4	10.7 ± 5.7	25.4 ± 4.3	11.5 ± 3.1	22.5 ± 4.9	27.1 ± 5.6
Basic - 75/25	50.9 ± 3.9	42.5 ± 4.0	33.7 ± 4.1	25.0 ± 4.1	17.2 ± 4.0	33.8 ± 3.9	15.2 ± 1.8	30.0 ± 2.8	33.7 ± 2.9
Basic - 50/50	44.5 ± 4.7	34.2 ± 5.0	23.8 ± 5.1	14.8 ± 4.7	7.9 ± 3.5	25.0 ± 4.3	11.7 ± 2.9	21.6 ± 4.0	25.6 ± 4.0
I3D_RGB+I3D_FLOW - 75/25	57.3 ± 3.6	47.8 ± 4.4	38.6 ± 4.9	28.6 ± 4.9	20.0 ± 4.7	38.5 ± 4.4	16.1 ± 2.0	32.0 ± 3.0	36.9 ± 3.1
I3D_RGB+I3D_FLOW - 50/50	49.3 ± 4.2	37.8 ± 6.2	26.6 ± 6.7	17.5 ± 6.2	10.8 ± 5.2	28.4 ± 5.7	11.4 ± 2.8	23.9 ± 5.6	28.1 ± 6.0

Table 13: Thumos Class-Agnostic Detection Results. Performance of class-agnostic detectors with different input features. mAP@0.5IoUs is the mean Average Precision at 0.5 Intersection over Union. mAP@avg is the average of mAP@0.3:0.1:0.7. AR@10 is Average Recall at 10. Aggregates are means ± standard error across splits.

Detection Model	Classification Model	Split(s)	mAP@0.5	mAP@0.75	mAP@avg
Clip b/32	Clip b/32	75/25	32.6 ± 0.6	18.7 ± 0.5	19.4 ± 0.4
Clip b/32	Clip b/32	Intermediate	34.7	20.4	21.0
Clip b/32	Clip b/32	Smart	36.7	22.4	22.6
Clip b/32	Clip b/32	50/50	30.1 ± 0.8	16.5 ± 0.5	17.3 ± 0.6
Clip b/16	Clip b/16	75/25	36.3 ± 0.7	20.7 ± 0.6	21.4 ± 0.5
Clip b/16	Clip b/16	Intermediate	38.6	22.7	23.4
Clip b/16	Clip b/16	Smart	38.1	22.6	23.4
Clip b/16	Clip b/16	50/50	33.3 ± 0.5	18.9 ± 0.5	19.5 ± 0.4
Clip l/14	Clip l/14	75/25	41.1 ± 0.6	23.8 ± 0.4	24.6 ± 0.4
Clip l/14	Clip l/14	Intermediate	43.0	24.8	25.7
Clip l/14	Clip l/14	Smart	45.0	27.7	28.7
Clip l/14	Clip l/14	50/50	38.7 ± 1.0	21.3 ± 0.7	22.4 ± 0.7
Align	Align	75/25	41.1 ± 1.0	23.2 ± 0.8	24.2 ± 0.7
Align	Align	Intermediate	45.0	25.5	26.9
Align	Align	Smart	45.2	27.1	28.1
Align	Align	50/50	39.2 ± 1.7	21.8 ± 1.0	22.9 ± 1.1
Basic	Basic	75/25	47.6 ± 0.6	27.5 ± 0.6	28.4 ± 0.5
Basic	Basic	Intermediate	48.7	28.8	29.4
Basic	Basic	Smart	50.4	30.7	31.2
Basic	Basic	50/50	45.8 ± 1.0	25.7 ± 0.8	26.4 ± 0.9
I3D_RGB+I3D_FLOW	Clip b/32	75/25	33.5 ± 0.6	19.7 ± 0.5	20.2 ± 0.4
I3D_RGB+I3D_FLOW	Clip b/32	Intermediate	34.9	21.3	21.5
I3D_RGB+I3D_FLOW	Clip b/32	Smart	38.3	23.2	23.9
I3D_RGB+I3D_FLOW	Clip b/32	50/50	30.2 ± 0.8	17.8 ± 0.7	18.2 ± 0.6
I3D_RGB+I3D_FLOW	Clip b/16	75/25	36.7 ± 0.6	21.5 ± 0.5	22.1 ± 0.5
I3D_RGB+I3D_FLOW	Clip b/16	Intermediate	38.1	23.0	23.2
I3D_RGB+I3D_FLOW	Clip b/16	Smart	38.2	23.6	24.1
I3D_RGB+I3D_FLOW	Clip b/16	50/50	33.4 ± 0.6	19.7 ± 0.6	20.1 ± 0.5
I3D_RGB+I3D_FLOW	Clip l/14	75/25	41.2 ± 0.5	24.2 ± 0.5	24.8 ± 0.4
I3D_RGB+I3D_FLOW	Clip l/14	Intermediate	42.1	25.7	25.8
I3D_RGB+I3D_FLOW	Clip l/14	Smart	44.3	27.7	28.1
I3D_RGB+I3D_FLOW	Clip l/14	50/50	38.1 ± 0.7	22.3 ± 0.7	22.8 ± 0.6
I3D_RGB+I3D_FLOW	Align	75/25	41.5 ± 0.9	24.1 ± 0.7	24.8 ± 0.6
I3D_RGB+I3D_FLOW	Align	Intermediate	43.7	26.4	26.6
I3D_RGB+I3D_FLOW	Align	Smart	45.1	27.8	28.4
I3D_RGB+I3D_FLOW	Align	50/50	38.4 ± 1.4	22.5 ± 1.1	22.9 ± 1.0
I3D_RGB+I3D_FLOW	Basic	75/25	47.0 ± 0.6	27.5 ± 0.5	28.2 ± 0.5
I3D_RGB+I3D_FLOW	Basic	Intermediate	48.2	29.0	29.3
I3D_RGB+I3D_FLOW	Basic	Smart	50.2	30.6	31.3
I3D_RGB+I3D_FLOW	Basic	50/50	44.2 ± 0.7	25.9 ± 0.8	26.4 ± 0.7
I3D_RGB+I3D_FLOW	MBT-v	75/25	39.5 ± 2.2	22.8 ± 1.7	23.4 ± 1.5
I3D_RGB+I3D_FLOW	MBT-v	Intermediate	40.0	23.7	24.0
I3D_RGB+I3D_FLOW	MBT-v	Smart	42.2	22.2	26.0
I3D_RGB+I3D_FLOW	MBT-v	50/50	36.0 ± 1.3	20.7 ± 1.1	21.1 ± 0.9

Table 14: ActivityNet Open Vocabulary Detection Results. performance of open-vocabulary temporal action detection for different combinations of class-agnostic detection features and open-vocabulary classification features. mAP@0.5IoUs is the mean Average Precision at 0.5 Intersection over Union. mAP@avg is the average of mAP@0.50:0.05:0.95. AR@10 is Average Recall at 10. Aggregates are means ± standard error across splits.

Detection Model	Classification Model	Split(s)	mAP@0.3	mAP@0.4	mAP@0.5	mAP@0.6	mAP@0.7	mAP@avg
Clip b/32	Clip b/32	75/25	21.4 ± 2.0	16.4 ± 1.8	11.8 ± 1.6	7.0 ± 1.2	3.5 ± 0.8	12.0 ± 1.4
Clip b/32	Clip b/32	50/50	15.4 ± 3.3	11.0 ± 2.4	7.7 ± 1.9	4.3 ± 1.3	1.9 ± 0.7	8.0 ± 1.8
Clip b/16	Clip b/16	75/25	21.8 ± 1.8	17.3 ± 1.7	13.2 ± 1.6	8.8 ± 1.6	3.7 ± 0.8	12.9 ± 1.3
Clip b/16	Clip b/16	50/50	18.0 ± 1.5	13.2 ± 1.1	8.9 ± 0.9	5.1 ± 0.9	2.2 ± 0.7	9.5 ± 0.8
Clip l/14	Clip l/14	75/25	28.6 ± 2.5	21.7 ± 2.0	15.4 ± 1.6	9.2 ± 1.2	4.2 ± 0.8	15.8 ± 1.6
Clip l/14	Clip l/14	50/50	21.0 ± 3.7	14.8 ± 2.4	9.8 ± 2.0	5.0 ± 1.1	2.0 ± 0.3	10.5 ± 1.9
Align	Align	75/25	15.1 ± 2.3	12.2 ± 2.0	8.9 ± 1.8	5.6 ± 1.7	1.7 ± 0.4	8.7 ± 1.5
Align	Align	50/50	12.8 ± 2.7	9.2 ± 1.9	6.1 ± 1.4	3.2 ± 0.7	1.1 ± 0.3	6.5 ± 1.4
Basic	Basic	75/25	36.6 ± 3.6	28.7 ± 3.1	20.6 ± 2.4	12.2 ± 1.7	5.9 ± 1.1	20.8 ± 2.3
Basic	Basic	50/50	30.5 ± 4.2	22.9 ± 3.8	15.9 ± 2.8	9.1 ± 2.2	4.2 ± 1.4	16.5 ± 2.7
I3D_RGB+I3D_FLOW	Clip b/32	75/25	25.1 ± 2.6	19.5 ± 2.2	13.9 ± 1.8	8.2 ± 1.3	4.0 ± 0.8	14.1 ± 1.7
I3D_RGB+I3D_FLOW	Clip b/32	50/50	21.0 ± 4.0	15.8 ± 3.3	11.3 ± 2.8	6.4 ± 2.1	3.0 ± 1.2	11.5 ± 2.6
I3D_RGB+I3D_FLOW	Clip b/16	75/25	27.8 ± 2.9	21.7 ± 2.6	15.3 ± 2.1	8.8 ± 1.4	4.3 ± 0.9	15.6 ± 1.9
I3D_RGB+I3D_FLOW	Clip b/16	50/50	23.6 ± 4.9	18.0 ± 4.0	12.8 ± 3.4	7.0 ± 2.4	3.2 ± 1.3	12.9 ± 3.1
I3D_RGB+I3D_FLOW	Clip l/14	75/25	30.1 ± 2.4	23.7 ± 2.3	16.8 ± 1.9	9.8 ± 1.4	4.7 ± 0.9	17.0 ± 1.7
I3D_RGB+I3D_FLOW	Clip l/14	50/50	26.1 ± 4.6	20.2 ± 4.2	14.3 ± 3.5	8.0 ± 2.6	3.6 ± 1.4	14.5 ± 3.2
I3D_RGB+I3D_FLOW	Align	75/25	19.1 ± 2.6	14.9 ± 2.1	10.0 ± 1.5	5.5 ± 0.9	2.4 ± 0.5	10.4 ± 1.5
I3D_RGB+I3D_FLOW	Align	50/50	15.5 ± 3.9	11.8 ± 2.9	8.2 ± 2.1	4.1 ± 1.1	1.8 ± 0.5	8.3 ± 2.1
I3D_RGB+I3D_FLOW	Basic	75/25	40.3 ± 3.0	31.8 ± 2.8	22.7 ± 2.4	13.3 ± 1.8	6.5 ± 1.1	22.9 ± 2.1
I3D_RGB+I3D_FLOW	Basic	50/50	35.3 ± 5.6	27.1 ± 6.0	19.3 ± 5.3	11.0 ± 3.9	5.0 ± 2.0	19.5 ± 4.6

Table 15: Thumos Open Vocabulary Detection Results. performance of open-vocabulary temporal action detection for different combinations of class-agnostic detection features and open-vocabulary classification features. mAP@0.5IoUs is the mean Average Precision at 0.5 Intersection over Union. mAP@avg is the average of mAP@0.3:0.1:0.7. Aggregates are means ± standard error across splits.

Model	mAP@0.5	mAP@0.75	mAP@0.95	mAP@avg	AR@10	AR@50	AR@100
Clip b/32							
+13D_FLOW - Intermediate	50.2	28.5	3.5	29.2	43.4	48.9	48.9
+13D_FLOW - Smart	53.0	29.7	3.0	30.6	44.2	47.2	47.2
+13D_RGB - Intermediate	48.8	28.2	3.6	28.8	43.1	48.2	48.2
+13D_RGB - Smart	51.2	30.5	3.7	30.7	44.6	47.3	47.3
+YAMNET - Intermediate	48.3	27.5	4.5	28.5	42.4	50.1	50.1
+YAMNET - Smart	50.3	29.4	5.4	30.3	44.6	49.2	49.2
+VGGISH - Intermediate	49.1	27.7	2.2	28.4	43.3	48.1	48.1
+VGGISH - Smart	50.1	28.9	3.8	29.7	43.3	49.4	49.4
+13D_FLOW+YAMNET - Intermediate	51.1	28.0	3.3	29.2	43.4	48.9	48.9
+13D_FLOW+YAMNET - Smart	52.0	30.2	3.6	31.0	45.7	49.6	49.6
+13D_FLOW+VGGISH - Intermediate	50.7	28.3	2.7	29.1	43.9	49.4	49.4
+13D_FLOW+VGGISH - Smart	52.9	30.6	4.0	31.5	44.7	49.3	49.3
+13D_FLOW+13D_RGB - Intermediate	49.7	27.6	2.9	28.6	43.7	48.2	48.2
+13D_FLOW+13D_RGB - Smart	52.7	29.3	3.9	30.8	42.1	49.5	49.5
+13D_FLOW+13D_RGB+YAMNET - Intermediate	51.2	28.8	3.1	29.8	45.1	49.7	49.7
+13D_FLOW+13D_RGB+YAMNET - Smart	52.6	31.0	3.7	31.5	46.0	50.7	50.7
+13D_FLOW+13D_RGB+VGGISH - Intermediate	49.1	28.8	4.0	29.2	44.2	49.0	49.0
+13D_FLOW+13D_RGB+VGGISH - Smart	53.1	29.8	4.2	30.9	44.5	48.1	48.1
Clip b/16							
+13D_FLOW - Intermediate	50.8	28.0	2.6	29.0	41.0	47.7	47.7
+13D_FLOW - Smart	52.8	29.9	3.3	30.9	44.8	48.8	48.8
+13D_RGB - Intermediate	48.7	27.4	3.1	28.4	43.2	48.6	48.6
+13D_RGB - Smart	51.1	29.5	4.1	30.5	44.6	49.3	49.3
+YAMNET - Intermediate	48.9	27.3	2.8	28.1	41.5	47.8	47.8
+YAMNET - Smart	51.2	29.3	5.0	30.3	44.1	48.1	48.1
+VGGISH - Intermediate	50.1	28.3	4.8	29.4	43.6	48.7	48.7
+VGGISH - Smart	51.3	30.5	6.0	31.1	44.8	50.6	50.6
+13D_FLOW+YAMNET - Intermediate	50.7	29.3	4.3	29.8	44.0	46.5	46.5
+13D_FLOW+YAMNET - Smart	52.8	31.1	4.9	31.5	43.9	48.4	48.4
+13D_FLOW+VGGISH - Intermediate	50.6	27.6	3.1	28.9	42.9	45.2	45.2
+13D_FLOW+VGGISH - Smart	52.8	30.5	2.7	31.2	44.0	48.1	48.1
+13D_FLOW+13D_RGB - Intermediate	50.8	28.4	3.1	29.3	42.9	46.9	46.9
+13D_FLOW+13D_RGB - Smart	52.1	29.4	3.6	30.6	46.1	49.9	49.9
+13D_FLOW+13D_RGB+YAMNET - Intermediate	50.3	28.1	4.3	29.4	44.5	49.3	49.3
+13D_FLOW+13D_RGB+YAMNET - Smart	52.1	30.1	4.6	30.9	41.3	48.7	48.7
+13D_FLOW+13D_RGB+VGGISH - Intermediate	51.6	28.9	3.8	29.9	44.5	49.5	49.5
+13D_FLOW+13D_RGB+VGGISH - Smart	51.7	30.5	3.1	31.0	44.8	49.8	49.8
Clip 1/4							
+13D_FLOW - Intermediate	49.7	28.1	3.3	29.0	42.5	47.8	47.8
+13D_FLOW - Smart	52.1	28.5	2.9	30.0	42.7	47.1	47.1
+13D_RGB - Intermediate	49.8	28.8	3.9	29.6	43.4	49.4	49.4
+13D_RGB - Smart	52.3	30.1	2.4	30.8	44.5	49.2	49.2
+YAMNET - Intermediate	49.7	28.7	5.2	29.5	44.8	48.8	48.8
+YAMNET - Smart	51.4	30.8	2.6	31.0	45.3	49.3	49.3
+VGGISH - Intermediate	49.7	29.3	4.3	29.8	43.7	50.5	50.5
+VGGISH - Smart	52.6	30.7	3.7	31.5	44.0	45.6	45.6
+13D_FLOW+YAMNET - Intermediate	48.5	27.9	4.5	28.7	42.2	47.9	47.9
+13D_FLOW+YAMNET - Smart	52.9	30.8	4.6	31.7	45.5	49.5	49.5
+13D_FLOW+VGGISH - Intermediate	51.2	29.4	3.6	30.2	44.8	48.4	48.4
+13D_FLOW+VGGISH - Smart	52.7	30.9	4.5	31.8	45.8	49.8	49.8
+13D_FLOW+13D_RGB - Intermediate	50.5	29.0	4.5	29.9	45.4	49.3	49.3
+13D_FLOW+13D_RGB - Smart	53.3	31.1	4.9	32.1	46.3	50.1	50.1
+13D_FLOW+13D_RGB+YAMNET - Intermediate	49.0	27.6	4.5	28.6	44.4	48.8	48.8
+13D_FLOW+13D_RGB+YAMNET - Smart	53.5	30.6	5.1	31.8	44.2	49.1	49.1
+13D_FLOW+13D_RGB+VGGISH - Intermediate	50.5	28.7	4.6	29.7	44.1	48.5	48.5
+13D_FLOW+13D_RGB+VGGISH - Smart	52.4	30.4	4.3	31.3	45.9	48.0	48.0
Align							
+13D_FLOW - Intermediate	51.0	28.8	2.8	29.4	43.9	48.1	48.1
+13D_FLOW - Smart	52.7	30.5	4.6	31.6	46.2	48.6	48.6
+13D_RGB - Intermediate	50.6	28.2	2.8	29.0	44.7	47.4	47.4
+13D_RGB - Smart	52.5	29.4	2.2	30.5	42.5	48.3	48.3
+YAMNET - Intermediate	49.6	27.6	3.3	28.4	42.3	48.6	48.6
+YAMNET - Smart	53.3	31.2	4.9	32.0	45.9	49.0	49.0
+VGGISH - Intermediate	50.3	29.3	3.6	29.3	43.9	48.8	48.8
+VGGISH - Smart	51.5	29.7	4.3	30.3	43.5	48.2	48.2
+13D_FLOW+YAMNET - Intermediate	49.1	27.8	4.3	29.0	43.3	48.2	48.2
+13D_FLOW+YAMNET - Smart	52.3	29.7	3.8	30.9	44.4	49.9	49.9
+13D_FLOW+VGGISH - Intermediate	49.3	28.2	4.3	29.3	44.3	45.6	45.6
+13D_FLOW+VGGISH - Smart	53.6	31.7	4.9	32.3	46.4	48.5	48.5
+13D_FLOW+13D_RGB - Intermediate	50.5	28.8	3.3	29.5	43.1	49.5	49.5
+13D_FLOW+13D_RGB - Smart	52.9	30.8	3.5	31.4	44.5	49.5	49.5
+13D_FLOW+13D_RGB+YAMNET - Intermediate	50.9	29.1	2.8	29.8	44.3	49.1	49.1
+13D_FLOW+13D_RGB+YAMNET - Smart	52.6	30.2	3.5	31.1	42.9	46.1	46.1
+13D_FLOW+13D_RGB+VGGISH - Intermediate	50.1	28.5	4.6	29.6	44.0	48.3	48.3
+13D_FLOW+13D_RGB+VGGISH - Smart	53.6	31.2	4.6	32.0	46.6	50.6	50.6
Basic							
+13D_FLOW - Intermediate	52.1	29.5	3.5	30.4	44.6	50.1	50.1
+13D_FLOW - Smart	54.0	31.1	4.3	32.2	46.6	50.1	50.1
+13D_RGB - Intermediate	50.9	28.6	3.9	29.8	44.7	50.8	50.8
+13D_RGB - Smart	53.3	30.3	3.6	31.2	44.7	50.3	50.3
+YAMNET - Intermediate	48.8	28.1	4.8	29.1	44.7	49.5	49.5
+YAMNET - Smart	52.9	31.1	5.2	32.1	45.2	49.9	49.9
+VGGISH - Intermediate	50.8	29.2	4.4	29.9	44.1	49.9	49.9
+VGGISH - Smart	53.6	31.3	4.3	31.9	46.4	48.9	48.9
+13D_FLOW+YAMNET - Intermediate	51.3	29.4	3.5	30.1	44.6	50.5	50.5
+13D_FLOW+YAMNET - Smart	54.2	32.6	5.0	33.0	46.2	48.8	48.8
+13D_FLOW+VGGISH - Intermediate	51.1	28.0	3.2	29.2	44.0	48.2	48.2
+13D_FLOW+VGGISH - Smart	54.6	31.3	4.2	32.2	45.8	50.4	50.4
+13D_FLOW+13D_RGB - Intermediate	51.1	28.1	2.9	29.5	45.2	49.6	49.6
+13D_FLOW+13D_RGB - Smart	53.8	30.8	3.8	31.9	44.8	49.3	49.3
+13D_FLOW+13D_RGB+YAMNET - Intermediate	51.7	28.5	3.2	30.0	45.1	47.8	47.8
+13D_FLOW+13D_RGB+YAMNET - Smart	53.5	30.9	5.4	32.2	46.2	49.0	49.0
+13D_FLOW+13D_RGB+VGGISH - Intermediate	51.4	28.3	3.4	29.7	44.0	49.4	49.4
+13D_FLOW+13D_RGB+VGGISH - Smart	54.5	30.5	3.7	31.8	45.9	49.2	49.2

Table 16: ActivityNet Class-Agnostic Detection Results for Feature Ensembles on a Subset of Splits. Performance of class-agnostic detectors with different input feature ensembles. mAP@0.5IoUs is the mean Average Precision at 0.5 Intersection over Union. mAP@avg is the average of mAP@0.50:0.05:0.95. AR@10 is Average Recall at 10. Aggregates are means \pm standard error across splits.

Model	mAP@0.5	mAP@0.75	mAP@0.95	mAP@avg	AR@10	AR@50	AR@100
Clip b/32							
+I3D_FLOW - 75/25	49.3 ± 0.7	27.3 ± 0.6	2.7 ± 0.2	28.2 ± 0.5	42.0 ± 0.5	47.6 ± 0.3	47.6 ± 0.3
+I3D_FLOW - Smart	53.0	29.7	3.0	30.6	44.2	47.2	47.2
+I3D_FLOW - 50/50	47.5 ± 0.9	25.6 ± 1.2	2.7 ± 0.5	26.8 ± 1.1	40.2 ± 1.4	45.1 ± 1.7	45.1 ± 1.7
+I3D_FLOW+VGGISH - 75/25	49.1 ± 0.6	27.3 ± 0.6	3.0 ± 0.2	28.2 ± 0.5	42.7 ± 0.4	47.4 ± 0.4	47.4 ± 0.4
+I3D_FLOW+VGGISH - Smart	52.9	30.6	4.0	31.5	44.7	49.3	49.3
+I3D_FLOW+VGGISH - 50/50	46.5 ± 0.8	25.8 ± 0.7	2.7 ± 0.2	26.6 ± 0.5	40.2 ± 0.6	45.9 ± 0.7	45.9 ± 0.7
+I3D_FLOW+I3D_RGB+VGGISH - 75/25	49.3 ± 0.7	27.6 ± 0.7	3.3 ± 0.2	28.5 ± 0.6	42.4 ± 0.6	47.3 ± 0.5	47.3 ± 0.5
+I3D_FLOW+I3D_RGB+VGGISH - Smart	53.1	29.8	4.2	30.9	44.5	48.1	48.1
+I3D_FLOW+I3D_RGB+VGGISH - 50/50	47.7 ± 0.3	26.1 ± 0.9	2.5 ± 0.3	27.0 ± 0.3	41.0 ± 0.3	46.3 ± 0.9	46.3 ± 0.9
Clip b/16							
+I3D_FLOW - 75/25	49.2 ± 0.5	27.3 ± 0.5	3.3 ± 0.2	28.4 ± 0.4	42.7 ± 0.5	47.6 ± 0.5	47.6 ± 0.5
+I3D_FLOW - Smart	52.8	29.9	3.3	30.9	44.8	48.8	48.8
+I3D_FLOW - 50/50	47.0 ± 0.9	25.6 ± 0.8	1.9 ± 0.6	26.4 ± 0.5	39.7 ± 0.7	45.4 ± 0.5	45.4 ± 0.5
+I3D_FLOW+VGGISH - 75/25	49.1 ± 0.5	27.4 ± 0.5	3.0 ± 0.1	28.3 ± 0.4	42.0 ± 0.4	46.8 ± 0.5	46.8 ± 0.5
+I3D_FLOW+VGGISH - Smart	52.8	30.5	2.7	31.2	44.0	48.1	48.1
+I3D_FLOW+VGGISH - 50/50	47.4 ± 0.9	25.2 ± 0.5	2.8 ± 0.1	26.6 ± 0.5	40.1 ± 1.1	46.0 ± 0.8	46.0 ± 0.8
+I3D_FLOW+I3D_RGB+VGGISH - 75/25	49.3 ± 0.6	28.0 ± 0.6	3.3 ± 0.2	28.9 ± 0.5	43.4 ± 0.6	47.9 ± 0.5	47.9 ± 0.5
+I3D_FLOW+I3D_RGB+VGGISH - Smart	51.7	30.5	3.1	31.0	44.8	49.8	49.8
+I3D_FLOW+I3D_RGB+VGGISH - 50/50	48.0 ± 0.7	25.9 ± 0.8	2.8 ± 0.4	27.1 ± 0.7	41.7 ± 1.2	46.3 ± 1.5	46.3 ± 1.5
Clip l/14							
+I3D_FLOW - 75/25	49.4 ± 0.5	27.7 ± 0.6	3.1 ± 0.3	28.6 ± 0.5	42.8 ± 0.4	47.3 ± 0.3	47.3 ± 0.3
+I3D_FLOW - Smart	52.1	28.5	2.9	30.0	42.7	47.1	47.1
+I3D_FLOW - 50/50	47.6 ± 1.0	25.7 ± 0.9	2.4 ± 0.4	26.8 ± 0.8	41.3 ± 0.6	46.3 ± 0.8	46.3 ± 0.8
+I3D_FLOW+VGGISH - 75/25	49.9 ± 0.6	27.8 ± 0.6	3.1 ± 0.3	28.8 ± 0.4	42.7 ± 0.5	46.9 ± 0.3	46.9 ± 0.3
+I3D_FLOW+VGGISH - Smart	52.7	30.9	4.5	31.8	45.8	49.8	49.8
+I3D_FLOW+VGGISH - 50/50	48.2 ± 0.4	26.7 ± 0.8	2.6 ± 0.1	27.6 ± 0.5	42.1 ± 0.3	46.9 ± 0.7	46.9 ± 0.7
+I3D_FLOW+I3D_RGB+VGGISH - 75/25	50.3 ± 0.6	28.0 ± 0.6	3.3 ± 0.2	29.0 ± 0.5	43.0 ± 0.5	48.2 ± 0.4	48.2 ± 0.4
+I3D_FLOW+I3D_RGB+VGGISH - Smart	52.4	30.4	4.3	31.3	45.9	48.0	48.0
+I3D_FLOW+I3D_RGB+VGGISH - 50/50	47.6 ± 0.6	26.0 ± 0.6	2.6 ± 0.2	27.0 ± 0.3	40.5 ± 0.9	45.9 ± 1.0	45.9 ± 1.0
Align							
+I3D_FLOW - 75/25	50.0 ± 0.6	28.5 ± 0.6	3.0 ± 0.2	29.1 ± 0.5	43.3 ± 0.5	47.9 ± 0.5	47.9 ± 0.5
+I3D_FLOW - Smart	52.7	30.5	4.6	31.6	46.2	48.6	48.6
+I3D_FLOW - 50/50	48.3 ± 1.1	27.4 ± 1.2	2.7 ± 0.6	28.0 ± 1.1	42.3 ± 1.4	46.8 ± 1.0	46.8 ± 1.0
+I3D_FLOW+VGGISH - 75/25	50.2 ± 0.6	28.2 ± 0.6	3.5 ± 0.3	29.2 ± 0.5	43.3 ± 0.5	47.5 ± 0.5	47.5 ± 0.5
+I3D_FLOW+VGGISH - Smart	53.6	31.7	4.9	32.3	46.4	48.5	48.5
+I3D_FLOW+VGGISH - 50/50	48.7 ± 0.2	26.5 ± 0.5	2.9 ± 0.2	27.7 ± 0.2	40.5 ± 1.1	45.6 ± 0.4	45.6 ± 0.4
+I3D_FLOW+I3D_RGB+VGGISH - 75/25	49.9 ± 0.7	28.2 ± 0.6	3.7 ± 0.3	29.1 ± 0.5	43.2 ± 0.5	47.8 ± 0.4	47.8 ± 0.4
+I3D_FLOW+I3D_RGB+VGGISH - Smart	53.6	31.2	4.6	32.0	46.6	50.6	50.6
+I3D_FLOW+I3D_RGB+VGGISH - 50/50	48.0 ± 1.1	26.5 ± 0.4	2.6 ± 0.3	27.5 ± 0.5	41.4 ± 1.3	46.3 ± 1.2	46.3 ± 1.2
Basic							
+I3D_FLOW - 75/25	50.0 ± 0.5	28.1 ± 0.6	2.9 ± 0.2	28.9 ± 0.5	43.5 ± 0.4	47.9 ± 0.6	47.9 ± 0.6
+I3D_FLOW - Smart	54.0	31.1	4.3	32.2	46.6	50.1	50.1
+I3D_FLOW - 50/50	48.2 ± 0.3	26.5 ± 0.8	2.9 ± 0.3	27.6 ± 0.5	42.3 ± 0.7	46.4 ± 1.0	46.4 ± 1.0
+I3D_FLOW+VGGISH - 75/25	49.6 ± 0.6	27.5 ± 0.6	3.2 ± 0.2	28.6 ± 0.5	43.1 ± 0.6	48.0 ± 0.4	48.0 ± 0.4
+I3D_FLOW+VGGISH - Smart	54.6	31.3	4.2	32.2	45.8	50.4	50.4
+I3D_FLOW+VGGISH - 50/50	48.5 ± 0.5	26.7 ± 0.7	2.6 ± 0.3	27.6 ± 0.5	42.5 ± 0.3	47.2 ± 0.4	47.2 ± 0.4
+I3D_FLOW+I3D_RGB+VGGISH - 75/25	49.7 ± 0.5	28.1 ± 0.5	3.3 ± 0.3	29.0 ± 0.5	43.7 ± 0.3	48.6 ± 0.6	48.6 ± 0.6
+I3D_FLOW+I3D_RGB+VGGISH - Smart	54.5	30.5	3.7	31.8	45.9	49.2	49.2
+I3D_FLOW+I3D_RGB+VGGISH - 50/50	47.5 ± 0.7	26.0 ± 0.6	2.4 ± 0.3	27.0 ± 0.3	41.0 ± 0.4	45.4 ± 0.7	45.4 ± 0.7

Table 17: ActivityNet Class-Agnostic Detection Results for Feature Ensembles. Performance of class-agnostic detectors with different input feature ensembles. mAP@0.5IoUs is the mean Average Precision at 0.5 Intersection over Union. mAP@avg is the average of mAP@0.50:0.05:0.95. AR@10 is Average Recall at 10. Aggregates are means ± standard error across splits.

Model	mAP@0.3	mAP@0.4	mAP@0.5	mAP@0.6	mAP@0.7	mAP@avg	AR@10	AR@50	AR@100
Clip b/32									
+I3D_FLOW - 75/25	43.3 ± 4.8	35.9 ± 4.3	27.6 ± 3.8	19.4 ± 3.5	12.2 ± 2.9	27.7 ± 3.7	11.9 ± 1.9	28.3 ± 2.4	35.9 ± 2.5
+I3D_FLOW - 50/50	45.9 ± 2.6	35.8 ± 3.2	25.4 ± 4.0	15.4 ± 3.9	8.2 ± 3.3	26.1 ± 3.2	10.5 ± 2.5	26.1 ± 4.2	31.6 ± 4.4
+I3D_FLOW+VGGISH - 75/25	48.3 ± 4.2	40.3 ± 4.3	30.8 ± 4.4	21.2 ± 4.2	13.4 ± 3.9	30.8 ± 4.1	13.6 ± 2.0	29.9 ± 2.5	35.4 ± 2.4
+I3D_FLOW+VGGISH - 50/50	47.7 ± 2.7	36.1 ± 3.5	24.5 ± 3.8	14.3 ± 3.7	7.3 ± 3.0	26.0 ± 3.1	10.4 ± 2.0	23.4 ± 3.2	28.5 ± 3.0
+I3D_FLOW+I3D_RGB+VGGISH - 75/25	53.1 ± 3.8	45.0 ± 3.9	35.1 ± 4.1	24.5 ± 4.2	15.4 ± 4.0	34.6 ± 3.9	13.8 ± 1.8	30.9 ± 2.4	36.6 ± 2.4
+I3D_FLOW+I3D_RGB+VGGISH - 50/50	48.1 ± 4.2	37.8 ± 4.3	26.3 ± 3.9	15.6 ± 3.7	7.8 ± 3.1	27.1 ± 3.6	10.6 ± 1.9	25.4 ± 2.8	30.8 ± 2.3
Clip b/16									
+I3D_FLOW - 75/25	50.3 ± 4.7	42.2 ± 4.9	33.2 ± 4.8	24.0 ± 4.6	15.3 ± 4.1	33.0 ± 4.5	13.8 ± 2.1	29.6 ± 2.4	35.9 ± 2.4
+I3D_FLOW - 50/50	47.9 ± 2.9	37.9 ± 3.6	27.1 ± 3.9	16.2 ± 3.9	8.1 ± 3.2	27.5 ± 3.4	10.7 ± 1.9	24.9 ± 3.4	30.8 ± 2.9
+I3D_FLOW+VGGISH - 75/25	53.2 ± 3.6	45.2 ± 3.7	35.8 ± 3.7	25.5 ± 3.7	16.4 ± 3.4	35.2 ± 3.4	14.5 ± 1.7	30.4 ± 2.1	35.9 ± 1.9
+I3D_FLOW+VGGISH - 50/50	43.5 ± 5.7	33.8 ± 5.3	23.1 ± 4.8	13.8 ± 4.2	6.9 ± 3.2	24.2 ± 4.5	9.5 ± 1.9	23.7 ± 2.6	29.7 ± 2.1
+I3D_FLOW+I3D_RGB+VGGISH - 75/25	58.8 ± 3.2	50.4 ± 3.6	40.8 ± 3.7	29.7 ± 3.8	19.6 ± 3.8	39.9 ± 3.5	16.1 ± 1.7	32.4 ± 2.3	38.0 ± 2.2
+I3D_FLOW+I3D_RGB+VGGISH - 50/50	44.9 ± 6.1	35.5 ± 6.1	25.9 ± 5.9	16.9 ± 5.2	9.9 ± 4.1	26.6 ± 5.5	11.0 ± 2.9	26.4 ± 3.0	32.1 ± 2.5
Clip l/14									
+I3D_FLOW - 75/25	58.1 ± 3.2	49.8 ± 3.5	39.7 ± 3.6	28.0 ± 3.4	17.5 ± 3.2	38.6 ± 3.2	15.1 ± 1.4	31.4 ± 2.1	36.5 ± 2.1
+I3D_FLOW - 50/50	50.2 ± 2.7	40.2 ± 4.1	28.8 ± 4.6	17.7 ± 4.1	9.1 ± 2.7	29.2 ± 3.5	11.4 ± 2.1	27.2 ± 3.5	31.9 ± 3.6
+I3D_FLOW+VGGISH - 75/25	59.4 ± 3.2	50.5 ± 3.7	40.5 ± 3.9	29.6 ± 4.0	19.7 ± 3.8	39.9 ± 3.6	16.2 ± 1.7	31.4 ± 2.3	36.8 ± 2.2
+I3D_FLOW+VGGISH - 50/50	49.0 ± 3.3	38.5 ± 3.7	27.6 ± 4.6	17.4 ± 4.8	9.7 ± 3.8	28.4 ± 4.0	11.3 ± 2.3	26.2 ± 4.2	32.2 ± 3.8
+I3D_FLOW+I3D_RGB+VGGISH - 75/25	52.2 ± 3.3	44.1 ± 3.3	33.8 ± 3.3	23.7 ± 3.3	14.9 ± 3.0	33.7 ± 3.1	13.9 ± 1.6	31.2 ± 2.5	37.2 ± 2.6
+I3D_FLOW+I3D_RGB+VGGISH - 50/50	46.2 ± 4.7	36.8 ± 4.4	26.6 ± 4.7	17.0 ± 4.3	9.3 ± 3.5	27.2 ± 4.2	11.4 ± 2.3	26.4 ± 3.7	31.5 ± 3.2
Align									
+I3D_FLOW - 75/25	57.2 ± 2.7	48.5 ± 2.9	38.4 ± 3.0	27.0 ± 2.9	17.5 ± 2.9	37.7 ± 2.6	15.7 ± 1.5	32.0 ± 2.0	37.3 ± 2.4
+I3D_FLOW - 50/50	49.8 ± 2.8	40.5 ± 3.7	29.8 ± 4.7	19.1 ± 4.7	11.1 ± 4.3	30.0 ± 4.0	12.3 ± 2.9	26.7 ± 4.2	32.2 ± 3.4
+I3D_FLOW+VGGISH - 75/25	46.1 ± 5.5	38.8 ± 5.2	30.4 ± 4.6	21.2 ± 3.8	13.0 ± 3.1	29.9 ± 4.3	12.0 ± 1.6	29.3 ± 2.0	36.8 ± 1.8
+I3D_FLOW+VGGISH - 50/50	28.4 ± 11.1	22.6 ± 9.5	16.5 ± 7.8	10.9 ± 5.7	6.1 ± 3.8	16.9 ± 7.6	6.2 ± 3.7	19.9 ± 5.5	29.9 ± 3.7
+I3D_FLOW+I3D_RGB+VGGISH - 75/25	56.7 ± 2.7	48.8 ± 2.9	38.9 ± 2.9	28.1 ± 3.0	18.3 ± 3.0	38.2 ± 2.7	15.8 ± 1.6	32.0 ± 2.0	37.4 ± 1.8
+I3D_FLOW+I3D_RGB+VGGISH - 50/50	47.8 ± 5.1	38.6 ± 4.8	27.3 ± 4.2	16.8 ± 3.7	8.8 ± 3.2	27.9 ± 3.7	11.3 ± 2.1	26.9 ± 3.6	32.4 ± 3.1
Basic									
+I3D_FLOW - 75/25	51.9 ± 4.1	43.0 ± 4.2	33.4 ± 4.2	23.3 ± 4.0	15.4 ± 3.9	33.4 ± 3.9	14.3 ± 2.1	29.7 ± 2.6	35.7 ± 2.5
+I3D_FLOW - 50/50	44.9 ± 7.0	35.5 ± 6.1	25.1 ± 5.3	15.4 ± 4.9	8.3 ± 3.9	25.9 ± 5.2	10.1 ± 2.8	24.1 ± 3.5	29.8 ± 2.9
+I3D_FLOW+VGGISH - 75/25	45.9 ± 4.7	38.1 ± 4.5	28.8 ± 4.1	19.5 ± 3.4	11.2 ± 2.6	28.7 ± 3.7	12.5 ± 1.6	29.7 ± 2.3	36.5 ± 2.6
+I3D_FLOW+VGGISH - 50/50	44.7 ± 2.0	35.1 ± 1.1	24.2 ± 1.6	13.9 ± 1.8	6.5 ± 1.4	24.9 ± 1.1	10.2 ± 1.1	25.3 ± 3.2	31.4 ± 3.0
+I3D_FLOW+I3D_RGB+VGGISH - 75/25	55.4 ± 3.4	46.7 ± 3.4	36.2 ± 3.5	25.3 ± 3.5	16.0 ± 3.2	35.9 ± 3.2	14.9 ± 1.3	31.1 ± 2.0	36.6 ± 2.5
+I3D_FLOW+I3D_RGB+VGGISH - 50/50	46.0 ± 4.0	36.5 ± 3.5	25.3 ± 3.8	15.6 ± 3.6	7.8 ± 2.6	26.2 ± 3.3	10.6 ± 2.0	26.1 ± 3.4	30.8 ± 3.4

Table 18: Thumos Class-Agnostic Detection Results for Feature Ensembles. Performance of class-agnostic detectors with different input feature ensembles. mAP@0.5IoUs is the mean Average Precision at 0.5 Intersection over Union. mAP@avg is the average of mAP@0.3:0.1:0.7. AR@10 is Average Recall at 10. Aggregates are means ± standard error across splits.

Added Features	Split(s)	mAP@0.5	mAP@0.75	mAP@avg
Clip b/32				
	75/25	32.6 ± 0.6	18.7 ± 0.5	19.4 ± 0.4
	Intermediate	34.7	20.4	21.0
	Smart	36.7	22.4	22.6
	50/50	30.1 ± 0.8	16.5 ± 0.5	17.3 ± 0.6
+I3D_FLOW +I3D_FLOW +I3D_FLOW +I3D_FLOW	75/25	33.0 ± 0.6	19.6 ± 0.6	19.9 ± 0.5
	Intermediate	35.2	21.6	21.8
	Smart	38.7	23.2	23.5
	50/50	30.1 ± 1.0	17.5 ± 1.1	18.0 ± 0.9
+I3D_FLOW+VGGISH +I3D_FLOW+VGGISH +I3D_FLOW+VGGISH +I3D_FLOW+VGGISH	75/25	32.8 ± 0.6	19.7 ± 0.6	20.0 ± 0.5
	Intermediate	35.7	21.9	21.9
	Smart	38.6	23.6	24.3
	50/50	29.7 ± 0.5	18.0 ± 0.6	18.1 ± 0.6
+I3D_FLOW+I3D_RGB+VGGISH +I3D_FLOW+I3D_RGB+VGGISH +I3D_FLOW+I3D_RGB+VGGISH +I3D_FLOW+I3D_RGB+VGGISH	75/25	33.1 ± 0.6	20.0 ± 0.6	20.2 ± 0.5
	Intermediate	35.1	22.1	22.1
	Smart	38.5	23.0	23.8
	50/50	30.3 ± 0.6	17.9 ± 0.9	18.0 ± 0.5
Clip b/16				
	75/25	36.3 ± 0.7	20.7 ± 0.6	21.4 ± 0.5
	Intermediate	38.6	22.7	23.4
	Smart	38.1	22.6	23.4
	50/50	33.3 ± 0.5	18.9 ± 0.5	19.5 ± 0.4
+I3D_FLOW +I3D_FLOW +I3D_FLOW +I3D_FLOW	75/25	36.4 ± 0.6	21.7 ± 0.6	22.1 ± 0.5
	Intermediate	38.3	22.7	23.0
	Smart	38.8	23.7	23.9
	50/50	33.5 ± nan	20.5 ± nan	20.7 ± nan
+I3D_FLOW+VGGISH +I3D_FLOW+VGGISH +I3D_FLOW+VGGISH +I3D_FLOW+VGGISH	75/25	36.1 ± 0.6	21.6 ± 0.5	22.0 ± 0.5
	Intermediate	38.1	22.4	23.0
	Smart	38.8	24.7	24.6
	50/50	33.1 ± 0.4	19.4 ± 0.3	19.9 ± 0.2
+I3D_FLOW+I3D_RGB+VGGISH +I3D_FLOW+I3D_RGB+VGGISH +I3D_FLOW+I3D_RGB+VGGISH +I3D_FLOW+I3D_RGB+VGGISH	75/25	36.6 ± 0.7	22.0 ± 0.7	22.4 ± 0.6
	Intermediate	39.0	23.4	24.1
	Smart	38.1	24.8	24.4
	50/50	34.0 ± 0.3	20.0 ± 0.4	20.5 ± 0.4
Clip l/14				
	75/25	41.1 ± 0.6	23.8 ± 0.4	24.6 ± 0.4
	Intermediate	43.0	24.8	25.7
	Smart	45.0	27.7	28.7
	50/50	38.7 ± 1.0	21.3 ± 0.7	22.4 ± 0.7
+I3D_FLOW +I3D_FLOW +I3D_FLOW +I3D_FLOW	75/25	40.8 ± 0.6	24.5 ± 0.6	24.8 ± 0.5
	Intermediate	42.1	25.9	26.3
	Smart	44.5	26.6	27.2
	50/50	38.3 ± 0.6	22.5 ± 0.7	22.9 ± 0.6
+I3D_FLOW+VGGISH +I3D_FLOW+VGGISH +I3D_FLOW+VGGISH +I3D_FLOW+VGGISH	75/25	41.0 ± 0.6	24.5 ± 0.6	24.8 ± 0.5
	Intermediate	43.4	26.8	27.0
	Smart	44.4	28.5	28.6
	50/50	38.8 ± 0.7	23.3 ± 0.9	23.6 ± 0.7
+I3D_FLOW+I3D_RGB+VGGISH +I3D_FLOW+I3D_RGB+VGGISH +I3D_FLOW+I3D_RGB+VGGISH +I3D_FLOW+I3D_RGB+VGGISH	75/25	41.1 ± 0.6	24.8 ± 0.6	25.1 ± 0.4
	Intermediate	42.3	26.3	26.5
	Smart	44.4	28.3	28.2
	50/50	38.2 ± 0.6	22.5 ± 0.7	22.9 ± 0.5
Align				
	75/25	41.1 ± 1.0	23.2 ± 0.8	24.2 ± 0.7
	Intermediate	45.0	25.5	26.9
	Smart	45.2	27.1	28.1
	50/50	39.2 ± 1.7	21.8 ± 1.0	22.9 ± 1.1
+I3D_FLOW +I3D_FLOW +I3D_FLOW +I3D_FLOW	75/25	41.5 ± 1.0	25.2 ± 0.8	25.3 ± 0.7
	Intermediate	44.4	27.5	27.2
	Smart	45.3	28.1	28.7
	50/50	39.1 ± 1.9	23.7 ± 1.6	23.9 ± 1.4
+I3D_FLOW+VGGISH +I3D_FLOW+VGGISH +I3D_FLOW+VGGISH +I3D_FLOW+VGGISH	75/25	41.4 ± 0.8	24.9 ± 0.9	25.3 ± 0.7
	Intermediate	43.2	27.1	27.1
	Smart	46.1	29.1	29.3
	50/50	39.3 ± 1.0	22.9 ± 1.0	23.6 ± 0.9
+I3D_FLOW+I3D_RGB+VGGISH +I3D_FLOW+I3D_RGB+VGGISH +I3D_FLOW+I3D_RGB+VGGISH +I3D_FLOW+I3D_RGB+VGGISH	75/25	41.2 ± 0.9	24.9 ± 0.8	25.3 ± 0.7
	Intermediate	43.9	27.8	27.8
	Smart	45.7	29.0	29.2
	50/50	38.7 ± 1.1	22.9 ± 0.8	23.4 ± 0.7
Basic				
	75/25	47.6 ± 0.6	27.5 ± 0.6	28.4 ± 0.5
	Intermediate	48.7	28.8	29.4
	Smart	50.4	30.7	31.2
	50/50	45.8 ± 1.0	25.7 ± 0.8	26.4 ± 0.9
+I3D_FLOW +I3D_FLOW +I3D_FLOW +I3D_FLOW	75/25	46.9 ± 0.6	28.4 ± 0.7	28.6 ± 0.5
	Intermediate	49.8	30.8	30.8
	Smart	51.2	31.6	32.1
	50/50	45.3 ± 0.5	27.0 ± 0.7	27.6 ± 0.5
+I3D_FLOW+VGGISH +I3D_FLOW+VGGISH +I3D_FLOW+VGGISH +I3D_FLOW+VGGISH	75/25	46.5 ± 0.6	27.8 ± 0.7	28.3 ± 0.5
	Intermediate	48.6	29.0	29.7
	Smart	51.0	31.6	32.0
	50/50	45.3 ± 0.2	27.0 ± 0.7	27.4 ± 0.5
+I3D_FLOW+I3D_RGB+VGGISH +I3D_FLOW+I3D_RGB+VGGISH +I3D_FLOW+I3D_RGB+VGGISH +I3D_FLOW+I3D_RGB+VGGISH	75/25	46.6 ± 0.5	28.4 ± 0.6	28.8 ± 0.5
	Intermediate	49.5	30.3	30.6
	Smart	51.6	31.3	32.1
	50/50	44.6 ± 0.8	26.8 ± 0.5	27.0 ± 0.4

Table 19: ActivityNet Open Vocabulary Detection Results with Feature Ensembles. performance of open-vocabulary temporal action detection for different combinations of class-agnostic detection features and the listed open-vocabulary classification features. mAP@0.5IoUs is the mean Average Precision at 0.5 Intersection over Union. mAP@avg is the average of mAP@0.50:0.05:0.95. Aggregates are means ± standard error across splits.

Added Features	Split(s)	mAP@0.3	mAP@0.4	mAP@0.5	mAP@0.6	mAP@0.7	mAP@avg
Clip b/32							
	75/25	21.4 ± 2.0	16.4 ± 1.8	11.8 ± 1.6	7.0 ± 1.2	3.5 ± 0.8	12.0 ± 1.4
	50/50	15.4 ± 3.3	11.0 ± 2.4	7.7 ± 1.9	4.3 ± 1.3	1.9 ± 0.7	8.0 ± 1.8
+I3D_FLOW	75/25	19.7 ± 2.8	16.0 ± 2.4	11.7 ± 1.8	7.0 ± 1.2	3.3 ± 0.7	11.5 ± 1.7
+I3D_FLOW	50/50	20.1 ± 2.6	15.3 ± 1.7	11.1 ± 1.5	6.3 ± 1.3	2.9 ± 1.0	11.1 ± 1.3
+I3D_FLOW+VGGISH	75/25	22.3 ± 2.5	17.5 ± 2.2	12.7 ± 1.7	7.5 ± 1.2	3.5 ± 0.7	12.7 ± 1.6
+I3D_FLOW+VGGISH	50/50	17.5 ± 5.2	13.0 ± 3.7	8.9 ± 2.5	4.8 ± 1.3	1.9 ± 0.4	9.2 ± 2.6
+I3D_FLOW+I3D_RGB+VGGISH	75/25	25.0 ± 2.7	19.4 ± 2.2	13.8 ± 1.8	7.8 ± 1.2	3.4 ± 0.7	13.9 ± 1.7
+I3D_FLOW+I3D_RGB+VGGISH	50/50	22.5 ± 1.8	16.8 ± 1.8	12.2 ± 2.1	7.3 ± 2.0	3.3 ± 1.4	12.4 ± 1.7
Clip b/16							
	75/25	21.8 ± 1.8	17.3 ± 1.7	13.2 ± 1.6	8.8 ± 1.6	3.7 ± 0.8	12.9 ± 1.3
	50/50	18.0 ± 1.5	13.2 ± 1.1	8.9 ± 0.9	5.1 ± 0.9	2.2 ± 0.7	9.5 ± 0.8
+I3D_FLOW	75/25	23.2 ± 1.9	17.8 ± 1.6	12.4 ± 1.3	7.2 ± 1.0	3.2 ± 0.6	12.8 ± 1.2
+I3D_FLOW	50/50	23.4 ± 2.7	17.4 ± 2.2	11.2 ± 1.7	6.0 ± 0.9	2.2 ± 0.4	12.0 ± 1.6
+I3D_FLOW+VGGISH	75/25	26.1 ± 3.0	20.6 ± 2.5	14.9 ± 2.0	8.9 ± 1.4	4.1 ± 0.8	14.9 ± 1.9
+I3D_FLOW+VGGISH	50/50	22.1 ± 3.9	16.1 ± 3.0	11.0 ± 2.2	6.2 ± 1.2	2.6 ± 0.5	11.6 ± 2.1
+I3D_FLOW+I3D_RGB+VGGISH	75/25	27.8 ± 3.1	22.3 ± 2.9	16.0 ± 2.3	9.5 ± 1.6	4.6 ± 0.9	16.0 ± 2.1
+I3D_FLOW+I3D_RGB+VGGISH	50/50	22.3 ± 3.0	16.5 ± 2.4	11.2 ± 1.9	5.8 ± 0.9	2.2 ± 0.3	11.6 ± 1.7
Clip l/14							
	75/25	28.6 ± 2.5	21.7 ± 2.0	15.4 ± 1.6	9.2 ± 1.2	4.2 ± 0.8	15.8 ± 1.6
	50/50	21.0 ± 3.7	14.8 ± 2.4	9.8 ± 2.0	5.0 ± 1.1	2.0 ± 0.3	10.5 ± 1.9
+I3D_FLOW	75/25	31.3 ± 2.2	24.6 ± 1.6	17.8 ± 1.3	10.4 ± 1.0	4.5 ± 0.6	17.7 ± 1.3
+I3D_FLOW	50/50	27.1 ± 1.3	19.7 ± 1.0	13.8 ± 1.0	7.9 ± 0.9	3.3 ± 0.6	14.4 ± 0.8
+I3D_FLOW+VGGISH	75/25	32.1 ± 2.2	26.3 ± 1.9	19.0 ± 1.4	10.9 ± 1.1	4.8 ± 0.7	18.6 ± 1.4
+I3D_FLOW+VGGISH	50/50	27.3 ± 3.2	20.6 ± 2.9	14.4 ± 2.5	8.2 ± 1.6	3.4 ± 0.9	14.8 ± 2.1
+I3D_FLOW+I3D_RGB+VGGISH	75/25	29.9 ± 2.3	23.4 ± 2.1	16.6 ± 1.9	9.9 ± 1.3	4.6 ± 0.9	16.9 ± 1.6
+I3D_FLOW+I3D_RGB+VGGISH	50/50	26.7 ± 3.7	20.2 ± 3.1	13.7 ± 2.3	7.8 ± 1.5	3.3 ± 0.7	14.3 ± 2.2
Align							
	75/25	15.1 ± 2.3	12.2 ± 2.0	8.9 ± 1.8	5.6 ± 1.7	1.7 ± 0.4	8.7 ± 1.5
	50/50	12.8 ± 2.7	9.2 ± 1.9	6.1 ± 1.4	3.2 ± 0.7	1.1 ± 0.3	6.5 ± 1.4
+I3D_FLOW	75/25	17.7 ± 2.4	13.5 ± 1.8	9.1 ± 1.3	4.9 ± 0.8	2.0 ± 0.4	9.4 ± 1.3
+I3D_FLOW	50/50	15.3 ± 3.3	11.1 ± 2.7	7.7 ± 2.1	4.2 ± 1.2	1.6 ± 0.4	8.0 ± 2.0
+I3D_FLOW+VGGISH	75/25	13.2 ± 1.9	10.0 ± 1.6	7.2 ± 1.2	4.1 ± 0.8	1.7 ± 0.3	7.2 ± 1.1
+I3D_FLOW+VGGISH	50/50	9.8 ± 4.4	7.1 ± 3.5	5.1 ± 2.6	2.6 ± 1.3	1.0 ± 0.5	5.1 ± 2.5
+I3D_FLOW+I3D_RGB+VGGISH	75/25	19.0 ± 2.7	14.6 ± 2.2	10.4 ± 1.7	5.6 ± 1.0	2.3 ± 0.5	10.4 ± 1.6
+I3D_FLOW+I3D_RGB+VGGISH	50/50	14.2 ± 3.1	10.7 ± 2.5	7.4 ± 2.0	3.9 ± 1.1	1.5 ± 0.5	7.6 ± 1.8
Basic							
	75/25	36.6 ± 3.6	28.7 ± 3.1	20.6 ± 2.4	12.2 ± 1.7	5.9 ± 1.1	20.8 ± 2.3
	50/50	30.5 ± 4.2	22.9 ± 3.8	15.9 ± 2.8	9.1 ± 2.2	4.2 ± 1.4	16.5 ± 2.7
+I3D_FLOW	75/25	33.2 ± 3.5	26.4 ± 3.3	18.6 ± 2.5	11.1 ± 1.8	5.1 ± 1.1	18.9 ± 2.4
+I3D_FLOW	50/50	23.7 ± 5.3	18.7 ± 4.4	13.0 ± 3.1	7.1 ± 1.9	2.9 ± 0.9	13.1 ± 3.0
+I3D_FLOW+VGGISH	75/25	35.2 ± 3.5	28.0 ± 3.1	20.0 ± 2.4	12.1 ± 1.6	5.4 ± 0.9	20.1 ± 2.2
+I3D_FLOW+VGGISH	50/50	35.2 ± 2.4	27.6 ± 2.4	19.2 ± 1.7	11.2 ± 1.3	4.9 ± 0.8	19.6 ± 1.6
+I3D_FLOW+I3D_RGB+VGGISH	75/25	37.2 ± 3.7	29.8 ± 3.2	21.1 ± 2.3	12.1 ± 1.4	5.3 ± 0.8	21.1 ± 2.2
+I3D_FLOW+I3D_RGB+VGGISH	50/50	32.8 ± 3.1	25.2 ± 3.4	17.6 ± 3.0	10.0 ± 2.1	4.1 ± 1.0	17.9 ± 2.5

Table 20: Thumos Open Vocabulary Detection Results with Feature Ensembles. Performance of open-vocabulary temporal action detection for different combinations of class-agnostic detection features and the listed open-vocabulary classification features. mAP@0.5IoUs is the mean Average Precision at 0.5 Intersection over Union. mAP@avg is the average of mAP@0.3:0.1:0.7. Aggregates are means ± standard error across splits.

Intermediate	r1	r2	r3	r4	r5
Zumba Putting on makeup Ironing clothes Discuss throw Doing karate Chopping wood Spinning Making a sandwich Playing bagpipes Brushing teeth Bungee jumping Vacuuming floor Fixing bicycle Wrapping presents Getting a tattoo Using uneven bars Playing piano Playing lacrosse Painting Polishing shoes Platform diving Sailing Belly dance Playing racquetball Tai chi Assembling bicycle Beach soccer Playing ten pins Calf roping Carving jack-o-lanterns Croquet Disc dog Elliptical trainer Futsal Hanging wallpaper Hurling Kneeling Making a cake Painting fence Playing beach volleyball Playing ice hockey Putting in contact lenses Removing ice from car Rollerblading Scuba diving Slacklining Sumo Table soccer Using the monkey bar Waxing skis	Drinking coffee Playing polo Cricket Bathing dog Preparing salad Playing saxophone Javelin throw Brushing hair Drinking beer Cleaning windows Starting a campfire Layup drill in basketball Shot put Skateboarding Preparing pasta Shaving High jump Getting a haircut Getting a piercing Hammer throw Hand washing clothes Windsurfing Mixing drinks Playing guitarra Tumbling Arm wrestling Baton twirling Blowing leaves Bullfighting Capoeira Clipping cat claws Decorating the Christmas tree Drum corps Fun sliding down Hand car wash Hula hoop Kite flying Longboarding Mooping floor Painting Playing drums Powerbocking Raking leaves Rock-paper-scissors Running a marathon Skiing Spread mulch Swinging at the playground Tug of war Waterskiing	Doing kickboxing Snatch Clean and jerk Playing field hockey Playing harmonica Washing face Ping-pong Playing water polo Cheerleading Playing flauta Triple jump Dodgeball Washing hands Using the balance beam Rock climbing Springboard diving Shaving legs Cumbia Mowing the lawn Ballnet Playing violin Hopscotch Removing curlers Kayaking Playing accordion BMX Beer pong Braiding hair Curling Changing car wheel Basket Doing a powerbomb Doing fencing Gargling mouthwash Having an ice cream Ice fishing Knitting Making a lemonade Painting furniture Playing blackjack Playing pool Putting on shoes Riding bumper cars Roof shingle removal Sharpening knives Snow tubing Surfing Throwing darts Using the rowing machine Welding	Tango Long jump Using parallel bars Grooming horse Pole vault Using the pommel horse Volleyball Cleaning shoes Paintball Tennis serve with ball bouncing Polishing furniture Doing nails Horseback riding Shoveling snow Smoking hookah Playing squash Smoking a cigarette Washing dishes Walking the dog Doing step aerobics Breakdancing Doing motocross Archery Playing kickball Playing badminton Baking cookies Blow-drying hair Building sandcastles Canoing Cutting the grass Doing crunches Fixing the roof Grooming dog Hitting a pinata Installing carpet Laying tile Making an omelette Peeling potatoes Doing step aerobics Playing rubik cube Rafting River tubing Rope skipping Shuffleboard Snowboarding Swimming Trimming branches or hedges Wakeboarding Applying sunscreen	Zumba Tango Putting on makeup Long jump Ironing clothes Using parallel bars Discuss throw Chopping wood Using the pommel horse Discuss throw Grooming horse Doing karate Pole vault Chopping wood Using the pommel horse Spinning Volleyball Making a sandwich Cleaning shoes Playing bagpipes Paintball Brushing teeth Tennis serve with ball bouncing Bungee jumping Polishing furniture Vacuuming floor Doing nails Fixing bicycle Horseback riding Wrapping presents Shoveling snow Getting a tattoo Smoking hookah Using uneven bars Playing squash Playing piano Smoking a cigarette Playing lacrosse Washing dishes Walking the dog Polishing shoes Doing step aerobics Platform diving Breakdancing Sailing Doing motocross Belly dance Archery Playing racquetball Playing kickball Tai chi Playing badminton	Drinking coffee Doing kickboxing Playing polo Snatch Cricket Clean and jerk Playing field hockey Playing harmonica Washing face Discuss throw Grooming horse Doing karate Pole vault Chopping wood Using the pommel horse Discuss throw Grooming horse Doing karate Pole vault Chopping wood Using the pommel horse Spinning Volleyball Making a sandwich Cleaning shoes Playing bagpipes Paintball Brushing teeth Tennis serve with ball bouncing Bungee jumping Polishing furniture Vacuuming floor Doing nails Fixing bicycle Horseback riding Wrapping presents Shoveling snow Getting a tattoo Smoking hookah Using uneven bars Playing squash Playing piano Smoking a cigarette Playing lacrosse Washing dishes Walking the dog Polishing shoes Doing step aerobics Platform diving Breakdancing Sailing Doing motocross Belly dance Archery Playing racquetball Playing kickball Tai chi Playing badminton Making a lemonade Making an omelette Mooping floor Painting fence Painting furniture Peeling potatoes Plastering Playing beach volleyball Playing blackjack Playing congas Playing drums Playing ice hockey Playing pool Putting in contact lenses Rafting Raking leaves Riding bumper cars River tubing Rollerblading Rope skipping Scuba diving Sharpening knives Shuffleboard Skiing Snow tubing Spread mulch Surfing Swimming Table soccer Trimming branches or hedges Using the monkey bar Wakeboarding Waxing skis Welding
r6	r7	r8	r9	r10	r11
Assembling bicycle Baking cookies Beach soccer Blow-drying hair Playing ten pins Building sandcastles Calf roping Canoing Carving jack-o-lanterns Cleaning sink Croquet Cutting the grass Disc dog Doing crunches Elliptical trainer Fixing the roof Futsal Grooming dog Hanging wallpaper Hitting a pinata Hurling Installing carpet Kneeling Laying tile Making a cake Making an omelette Painting fence Peeling potatoes Playing beach volleyball Playing ice hockey Putting in contact lenses Rafting Removing ice from car River tubing Rollerblading Rope skipping Scuba diving Shuffleboard Slacklining Sumo Swimming Table soccer Trimming branches or hedges Using the monkey bar Wakeboarding Waxing skis	Arm wrestling BMX Baton twirling Beer pong Blowing leaves Braiding hair Bullfighting Camel ride Capoeira Changing car wheel Clipping cat claws Decorating the Christmas tree Drum corps Fun sliding down Gargling mouthwash Hand car wash Having an ice cream Hula hoop Ice fishing Kite flying Knitting Longboarding Making a lemonade Mooping floor Painting furniture Plastering Playing blackjack Playing drums Playing pool Powerbocking Putting on shoes Raking leaves Riding bumper cars Rock-paper-scissors Running a marathon Sharpening knives Skiing Snow tubing Spread mulch Surfing Swinging at the playground Tug of war Waterskiing	Drinking coffee Zumba Doing kickboxing Tango Playing polo Putting on makeup Snatch Long jump Cricket Ironing clothes Cleaning shoes Using parallel bars Bathing dog Discuss throw Playing field hockey Grooming horse Preparing salad Doing karate Playing harmonica Pole vault Playing saxophone Chopping wood Washing face Using the pommel horse Javelin throw Spinning Ping-pong Volleyball Brushing hair Making a sandwich Playing water polo Cleaning shoes Drinking beer Playing bagpipes Cheerleading Paintball Cleaning windows Brushing teeth Playing flauta Tennis serve with ball bouncing Starting a campfire Bungee jumping Triple jump Polishing furniture Layup drill in basketball Vacuuming floor Dodgeball Doing nails Shot put	Washing hands Horseback riding Skateboarding Wrapping presents Using the balance beam Shoveling snow Preparing pasta Getting a tattoo Rock climbing Smoking hookah Shaving Using uneven bars Springboard diving Playing squash High jump Playing piano Shaving legs Smoking a cigarette Getting a haircut Playing lacrosse Cumbia Washing dishes Getting a piercing Painting Mowing the lawn Walking the dog Hammer throw Polishing shoes Ballet Doing step aerobics Hand washing clothes Fixing the roof Playing violin Breakdancing Windsurfing Sailing Hopscotch Doing motocross Mixing drinks Belly dance Removing curlers Archery Playing guitarra Playing racquetball Playing kickball Tumbling Tai chi Playing accordion	Arm wrestling Assembling bicycle BMX Baking cookies Baton twirling Beach soccer Beer pong Blow-drying hair Blowing leaves Braiding hair Bullfighting Camel ride Changing car wheel Clipping cat claws Curling Cutting the grass Decorating the Christmas tree Disc dog Doing a powerbomb Doing crunches Fun sliding down Futsal Grooming dog Hanging wallpaper Hitting a pinata Hula hoop Hurling Installing carpet Kneeling Kite flying Knitting Longboarding Making a lemonade Mooping floor Painting furniture Plastering Playing beach volleyball Playing blackjack Playing congas Playing drums Playing ice hockey Playing pool Putting in contact lenses Rafting Elliptical trainer Doing fencing Doing step aerobics Platform diving Breakdancing Sailing Doing motocross Belly dance Archery Playing racquetball Playing kickball Tai chi Playing badminton Cleaning sink Clipping cat claws Croquet Curling Cutting the grass Decorating the Christmas tree Disc dog Doing a powerbomb Doing crunches Fun sliding down Futsal Gargling mouthwash Grooming dog Hand car wash Hitting a pinata Hula hoop Hurling Ice fishing Installing carpet Kite flying Knitting Longboarding Making a lemonade Mooping floor Painting furniture Plastering Playing beach volleyball Playing blackjack Playing congas Playing drums Playing ice hockey Playing pool Putting in contact lenses Rafting Raking leaves Riding bumper cars River tubing Rollerblading Rope skipping Scuba diving Sharpening knives Shuffleboard Skiing Snow tubing Spread mulch Surfing Swimming Table soccer Trimming branches or hedges Using the monkey bar Wakeboarding Waxing skis Welding	Arm wrestling Assembling bicycle BMX Baking cookies Baton twirling Beach soccer Beer pong Blow-drying hair Blowing leaves Braiding hair Bullfighting Camel ride Changing car wheel Clipping cat claws Curling Cutting the grass Decorating the Christmas tree Disc dog Doing a powerbomb Doing crunches Fun sliding down Futsal Gargling mouthwash Grooming dog Hand car wash Hitting a pinata Hula hoop Hurling Ice fishing Installing carpet Kite flying Knitting Longboarding Making a lemonade Mooping floor Painting furniture Plastering Playing beach volleyball Playing blackjack Playing congas Playing drums Playing ice hockey Playing pool Putting in contact lenses Rafting Raking leaves Riding bumper cars River tubing Rollerblading Rope skipping Scuba diving Sharpening knives Shuffleboard Skiing Snow tubing Spread mulch Surfing Swimming Table soccer Trimming branches or hedges Using the monkey bar Wakeboarding Waxing skis Welding

Table 21: ActivityNet 75/25 random splits. The strings listed are the ActivityNet labels held out for evaluation. The first column is the Intermediate split mentioned in the main text.

r0	r1	r2	r3
Zumba	Drinking coffee	Drinking coffee	Arm wrestling
Tango	Doing kickboxing	Zumba	Assembling bicycle
Putting on makeup	Playing polo	Doing kickboxing	BMX
Long jump	Snatch	Tango	Baking cookies
Ironing clothes	Cricket	Playing polo	Baton twirling
Using parallel bars	Clean and jerk	Putting on makeup	Beach soccer
Discus throw	Bathing dog	Snatch	Beer pong
Grooming horse	Playing field hockey	Long jump	Blow-drying hair
Doing karate	Preparing salad	Cricket	Blowing leaves
Pole vault	Playing harmonica	Ironing clothes	Playing ten pins
Chopping wood	Playing saxophone	Clean and jerk	Braiding hair
Using the pommel horse	Washing face	Using parallel bars	Building sandcastles
Spinning	Javelin throw	Bathing dog	Bullfighting
Volleyball	Ping-pong	Discus throw	Calf roping
Making a sandwich	Brushing hair	Playing field hockey	Camel ride
Cleaning shoes	Playing water polo	Grooming horse	Canoeing
Playing bagpipes	Drinking beer	Preparing salad	Capoeira
Paintball	Cheerleading	Doing karate	Carving jack-o-lanterns
Brushing teeth	Cleaning windows	Playing harmonica	Changing car wheel
Tennis serve with ball bouncing	Playing flauta	Pole vault	Cleaning sink
Bungee jumping	Starting a campfire	Playing saxophone	Clipping cat claws
Polishing furniture	Triple jump	Chopping wood	Croquet
Vacuuming floor	Layup drill in basketball	Washing face	Curling
Doing nails	Dodgeball	Using the pommel horse	Cutting the grass
Fixing bicycle	Shot put	Javelin throw	Decorating the Christmas tree
Horseback riding	Washing hands	Spinning	Disc dog
Wrapping presents	Skateboarding	Ping-pong	Doing a powerbomb
Shoveling snow	Using the balance beam	Volleyball	Doing crunches
Getting a tattoo	Preparing pasta	Brushing hair	Drum corps
Smoking hookah	Rock climbing	Making a sandwich	Elliptical trainer
Using uneven bars	Shaving	Playing water polo	Doing fencing
Playing squash	Sprintboard diving	Cleaning shoes	Fixing the roof
Playing piano	High jump	Drinking beer	Fun sliding down
Smoking a cigarette	Shaving legs	Playing bagpipes	Futsal
Playing lacrosse	Getting a haircut	Cheerleading	Gargling mouthwash
Washing dishes	Cumbia	Paintball	Grooming dog
Painting	Getting a piercing	Cleaning windows	Hand car wash
Walking the dog	Mowing the lawn	Brushing teeth	Hanging wallpaper
Polishing shoes	Hammer throw	Playing flauta	Having an ice cream
Doing step aerobics	Ballet	Tennis serve with ball bouncing	Hitting a pinata
Platform diving	Hand washing clothes	Starting a campfire	Hula hoop
Breakdancing	Playing violin	Bungee jumping	Hurling
Sailing	Windsurfing	Triple jump	Ice fishing
Doing motocross	Hopscotch	Polishing furniture	Installing carpet
Belly dance	Mixing drinks	Layup drill in basketball	Kite flying
Archery	Removing curlers	Vacuuming floor	Kneeling
Playing racquetball	Playing guitarra	Dodgeball	Knitting
Playing kickball	Kayaking	Doing nails	Laying tile
Tai chi	Tumbling	Shot put	Longboarding
Playing badminton	Playing accordion	Fixing bicycle	Making a cake
Assembling bicycle	Arm wrestling	Washing hands	Making a lemonade
Baking cookies	BMX	Horseback riding	Making an omelette
Beach soccer	Baton twirling	Skateboarding	Mopping floor
Blow-drying hair	Beer pong	Wrapping presents	Painting fence
Playing ten pins	Blowing leaves	Using the balance beam	Painting furniture
Building sandcastles	Braiding hair	Shoveling snow	Peeling potatoes
Calf roping	Bullfighting	Preparing pasta	Plastering
Canoeing	Camel ride	Getting a tattoo	Playing beach volleyball
Carving jack-o-lanterns	Capoeira	Rock climbing	Playing blackjack
Cleaning sink	Changing car wheel	Smoking hookah	Playing congas
Croquet	Clipping cat claws	Shaving	Playing drums
Cutting the grass	Curling	Using uneven bars	Playing ice hockey
Disc dog	Decorating the Christmas tree	Sprintboard diving	Playing pool
Doing crunches	Doing a powerbomb	Playing squash	Playing rubik cube
Elliptical trainer	Drum corps	High jump	Powerbocking
Fixing the roof	Doing fencing	Playing piano	Putting in contact lenses
Futsal	Fun sliding down	Shaving legs	Putting on shoes
Grooming dog	Gargling mouthwash	Smoking a cigarette	Rafting
Hanging wallpaper	Hand car wash	Getting a haircut	Raking leaves
Hitting a pinata	Having an ice cream	Playing lacrosse	Removing ice from car
Hurling	Hula hoop	Cumbia	Riding bumper cars
Installing carpet	Ice fishing	Washing dishes	River tubing
Knocking	Kite flying	Getting a piercing	Rock-paper-scissors
Laying tile	Knitting	Painting	Rollerblading
Making a cake	Longboarding	Mowing the lawn	Roof shingle removal
Making an omelette	Making a lemonade	Walking the dog	Rope skipping
Painting fence	Mopping floor	Hammer throw	Running a marathon
Peeling potatoes	Painting furniture	Polishing shoes	Scuba diving
Playing beach volleyball	Plastering	Ballet	Sharpening knives
Playing congas	Playing blackjack	Doing step aerobics	Shuffleboard
Playing ice hockey	Playing drums	Hand washing clothes	Skiing
Playing rubik cube	Playing pool	Platform diving	Slacklining
Putting in contact lenses	Powerbocking	Playing violin	Snow tubing
Rafting	Putting on shoes	Breakdancing	Snowboarding
Removing ice from car	Raking leaves	Windsurfing	Spread mulch
River tubing	Riding bumper cars	Sailing	Sumo
Rollerblading	Rock-paper-scissors	Hopscotch	Surfing
Rope skipping	Roof shingle removal	Doing motocross	Swimming
Scuba diving	Running a marathon	Mixing drinks	Swinging at the playground
Shuffleboard	Sharpening knives	Belly dance	Table soccer
Slacklining	Skiing	Removing curlers	Throwing darts
Snowboarding	Snow tubing	Archery	Trimming branches or hedges
Sumo	Spread mulch	Playing guitarra	Tug of war
Swimming	Surfing	Playing racquetball	Using the monkey bar
Swinging at the playground	Swinging at the playground	Kayaking	Using the rowing machine
Trimming branches or hedges	Throwing darts	Playing kickball	Wakeboarding
Using the monkey bar	Tug of war	Tumbling	Waterskiing
Wakeboarding	Using the rowing machine	Tai chi	Waxing skis
Waxing skis	Waterskiing	Playing accordion	Welding
Applying sunscreen	Welding	Playing badminton	Applying sunscreen

Table 22: ActivityNet 50/50 random splits. The strings listed are the ActivityNet labels held out for evaluation.

r0	r1	r2	r3	r4	r5
BaseballPitch CliffDiving FrisbeeCatch JavelinThrow SoccerPenalty	BasketballDunk CricketBowling GolfSwing LongJump TennisSwing	Billiards CricketShot HammerThrow PoleVault ThrowDiscus	CleanAndJerk Diving HighJump Shotput VolleyballSpiking	BasketballDunk CleanAndJerk CricketBowling Diving GolfSwing	BaseballPitch Billiards CliffDiving CricketShot FrisbeeCatch
r6	r7	r8	r9	r10	r11
HighJump LongJump Shotput TennisSwing VolleyballSpiking	HammerThrow JavelinThrow PoleVault SoccerPenalty ThrowDiscus	BaseballPitch BasketballDunk Billiards CleanAndJerk CliffDiving	CricketBowling CricketShot Diving FrisbeeCatch GolfSwing	HammerThrow HighJump JavelinThrow LongJump PoleVault	Shotput SoccerPenalty TennisSwing ThrowDiscus VolleyballSpiking

Table 23: Thumos 75/25 random splits. The strings listed are the Thumos labels held out for evaluation.

r0	r1	r2	r3
BasketballDunk CleanAndJerk CricketBowling Diving GolfSwing HighJump LongJump Shotput TennisSwing VolleyballSpiking	BaseballPitch Billiards CliffDiving CricketShot FrisbeeCatch HammerThrow JavelinThrow PoleVault SoccerPenalty ThrowDiscus	BaseballPitch BasketballDunk Billiards CleanAndJerk CliffDiving CricketBowling CricketShot Diving FrisbeeCatch GolfSwing	HammerThrow HighJump JavelinThrow LongJump PoleVault Shotput SoccerPenalty TennisSwing ThrowDiscus VolleyballSpiking

Table 24: Thumos 50/50 random splits. The strings listed are the Thumos labels held out for evaluation.